Journal of Cleaner Production 457 (2024) 142482

Contents lists available at ScienceDirect

Journal of Cleaner Production

journal homepage: www.elsevier.com/locate/jclepro

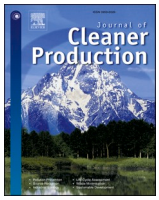

Towards artificial intelligence empowered performance enhancement of EDM process using nano-graphene mixed bio-dielectric supporting the carbon neutrality and sustainable development

Kashif Ishfaq [a,**], Muhammad Asad [a], Waqar Muhammad Ashraf [b], Muhammad Sana [a], Saqib Anwar [c], Wei Zhang [d], Vivek Dua [b,*]

[a] Department of Industrial and Manufacturing Engineering, Faculty of Mechanical Engineering, University of Engineering and Technology Lahore 54890, Pakistan
[b] The Sargent Centre for Process Systems Engineering, Department of Chemical Engineering, University College London, Torrington Place, London, WC1E 7JE, UK
[c] Industrial Engineering Department, College of Engineering, King Saud University, P.O. Box 800, Riyadh, 11421, Saudi Arabia
[d] School of Environmental Science and Engineering, Guangzhou University, Guangzhou, 510006, PR China

ARTICLE INFO

Handling editor: Kathleen Aviso

Keywords:
EDM
Ti–6Al–4V
Sustainable machining
Dielectric fluid
Nano graphene
Rice bran oil

ABSTRACT

The growing population with every passing day sets an alarming situation with respect to the conservation climate protocols. The increasing needs of society also demand a significant enhancement in the manufacturing capacity to augment the situation. However, it's a stringent requirement of the hour to propose sustainable and clean manufacturing processes to realize the goal of carbon neutrality to support a healthy life on the earth. Specifically, the processes that are energy intensive like electric discharge machining (EDM) are of serious concern regarding sustainability viewpoint. The role of the said process cannot be essentially eliminated as advent of new materials of superior characteristics demand the application of EDM for accurate cutting of intricate profiles. Nevertheless, the commonly used oil-based dielectric (kerosene) in EDM releases aerosol, deposit particles, oxides of carbon (CO_2 & CO), thus contributing to the environmental contamination. It is pertinent to mention that industries are compelled to tune their processes to achieve the goals of Net-Zero. Therefore, this study thoroughly investigates the potential of nano-graphene mixed rice bran oil to make the EDM process cleaner and sustainable which has never been investigated so far. Moreover, the process has been successfully modeled using artificial neural network (ANN) and optimized by non-dominated sorting genetic algorithm-II (NSGA-II) which is another novel aspect of this study as it eradicates the need of extensive experimentation. Experimentation has been performed via Taguchi's experimental strategy followed by a detailed explanation of the findings based on process physics. In comparison to the traditional dielectric an improvement of 98.8% in material removal rate (MRR) and 93.9% reduction in specific energy consumption (SEC) are realized if the said novel combination is applied without compromising the quality. CO_2 emissions determined for both rice bran oil and kerosene oil have revealed that rice bran oil provides 99.96% lesser CO_2 emission in comparison to its counterpart.

1. Introduction

The demand of high-strength alloys, especially Ti–6Al–4V, is being increased in various applications like bio-engineering, automotive, aerospace, aircraft, and marine productions, owing to its exclusive physical features (Tharian et al., 2022). The machining of said titanium (Ti) material using traditional processes is really challenging because the tool is directly contacted with the workpiece during the cutting operation. As a result, chattering, vibrations, and thermo-mechanical stresses are induced into the workpiece, which can drop the strength of the material (Ishfaq et al., 2023a; Papazoglou et al., 2021). Therefore, researchers diverted their focus from conventional machining to unconventional cutting processes. Amongst various unconventional techniques, electric discharge machining (EDM) is commonly preferred. The

* Corresponding author.
** Corresponding author.
E-mail addresses: kashif.ishfaq@uet.edu.pk (K. Ishfaq), 2016IM11@student.uet.edu.pk (M. Asad), Waqar.ashraf.21@ucl.ac.uk (W.M. Ashraf), 2016IM15@student.uet.edu.pk (M. Sana), sanwar@ksu.edu.sa (S. Anwar), zh_wei@gzhu.edu.cn (W. Zhang), v.dua@ucl.ac.uk (V. Dua).

https://doi.org/10.1016/j.jclepro.2024.142482
Received 23 November 2023; Received in revised form 30 April 2024; Accepted 3 May 2024
Available online 6 May 2024

popularity of the EDM process in different production industries is due to its unique and special qualities. Such as (i) it can easily handle/-machine hard-to-cut materials, (ii) the potency of the material is also not altered due to no connection between the electrode and the specimen, (iii) it can generate intricate and near-net shapes on the workpiece irrespective of considering the mechanical attributes (Philip et al., 2021; Perumal et al., 2021).

EDM operates on the principle of electro-thermal energy, which generates repetitive sparks within a dielectric pool present between the electrode and work part (Sana et al., 2023a). This makes strong pulse discharges and develops a plasma channel that causes undesirable erosion from the specimen's surface. As an action, the temperature goes to more than 12,000 °C (Sana et al., 2023b). During this process, debris/melted particles are usually flushed away by dielectric fluid. Besides involving in the flushing activity, dielectric fluid has manifold functions: it absorbs heat energy during sparking, stays electrically insulator till the breakdown voltage is not achieved, and works like a coolant (Das et al., 2021). Normally, in the EDM process, kerosene oil or deionized water is employed as a conventional insulating medium as claimed by Garg and Lam (2016). However, these dielectrics liberate harmful fumes, vapors, and toxic gases while machining. It will not only be affected the environment but also disturbs the operator's health (Singh et al., 2018; Leppert, 2018). Since, kerosene oil falls in the class of hydrocarbon-based dielectric, it yields more carbon footprints as compared to other dielectrics during EDM process. This occurs because of inherent characteristics of kerosene oil, i.e., high flammability, poor biodegradability, and low viscosity (Muttamara and Kanchanomai, 2016). In addition, the key factor behind the change in climate and global warming is the increase in carbon footprints. This booms the earth's temperature and result in the loss of sustainable manufacturing (Chukka et al., 2022).

According to department of commerce (USA), sustainable manufacturing is defined as "the fabrication of manufacturing goods by utilizing such processes which conserve energy, produce minimal wastes, reduce environmental impacts, and are ecological, economical, nontoxic and sound for all the communities" (Valaki et al., 2019). Thus, in order to make the EDM process fully sustainable, harmless, cost-effective, and energy conservative, different researchers proposed solutions to the previously described issues belonging to traditional EDM. Muthuramalingam and Mohan (2015) said that hazardous particles generated while standard EDM process can be omitted by using green dielectric fluids. R. et al. (S et al., 2021) demonstrated that environmental pollution and human diseases are enormously decreased when biodegradable oils used instead of hydrocarbon based dielectrics such as kerosene oil. Singaravel et al. (2020) illustrated that vegetable oil mixed dielectric medium is an effective substitute of kerosene oil for attaining sustainable and environment friendly EDM. The similar solutions were also suggested by different researchers (Rajurkar et al., 2017; Ming et al., 2021). In a study conducted on EDM of Inconel it was claimed that more than 5 times increase in MRR can be achieved if amla oil is used as dielectric instead of kerosene (Ishfaq et al., 2023b). Since, biodegradable oils have high sustainability index and thus it could be a reliable alternative to conventional dielectric oil (Valaki et al., 2019). Thereof, the current research utilized a biodegradable oil (rice bran oil (RBO)) as dielectric fluid. RBO is also called "healthy oil" due to existence of fatty acids in a well-balanced form. The aforesaid oil has wide acceptance in applications like pharmaceutical, cosmetics, food, polymer, and fuel industries. Such a tremendous use of RBO in wide range of applications is mainly because of its inimitable characteristics including anti-allergic, anti-flammable, anti-toxic, high biodegradability, and anti-carcinogenicity (Fraterrigo et al., 2021; Punia et al., 2021). Hence, RBO is a well-matched candidate for the cutting of employed titanium material through EDM setup.

Besides considering the impact of dielectric, Pradhan (2013) revealed that using optimum values of design variables is important to reducing the atmospheric impacts that result from the EDM operation. They also evaluated that improving environmental consequences may affect the manufacturing ingredients like material removal rate (MRR), tool wear rate (TWR), surface roughness (SR), specific energy consumption (SEC), and dimensional overcut (OC). Manufacturing sectors always seek a great equilibrium between manufacturing ingredients and environmental facets (Garg and Lam, 2016). Additionally, all the mentioned responses are prime variables of the EDM process because they describe the process's effectiveness, sustainability, and efficiency. Such as, MRR decides the economic state of the process, TWR is a pre-requisite of dimensional accuracy, SR is principally needed to achieve a good surface finish, SEC illustrates the consumption of energy, and OC justifies the proper functionality of the finished products. Thus, energy-conscious, cost-effective, and sustainable EDM can be achieved by improving these responses (Arif et al., 2022). To develop machined cuts over the Ti–6Al–4V, the current research has assayed effectiveness of green EDM in terms of MRR, SR, and SEC.

Significant literature is found where investigators have deliberated the impact of different EDM factors on the responses by utilizing biodegradable dielectric(s). For instance, Chakraborty et al. (2023) inspected the feasibility of EDM oil, rice bran biodiesel oil (BD) and jatropha biodiesel oil while EDM of Al6063. They evaluated MRR and SR against peak current (I_p), pulse on-time (T_{on}), and gap voltage (V_G). Researchers noted that jatropha BD has a finer surface finish than rice bran BD. In the context of MRR, both vegetable oils provided high magnitude followed by EDM oil at high value of I_p and V_G. Valaki et al. (2016) reported that MRR is 38% improved by the EDM process under palm oil dielectric than that of kerosene oil when current (I), duty factor, and T_{on} were set at 12 A, 50%, and 200 μsec, respectively. However, they have noted the same SR with both the dielectrics. The effect of Polanga bio-oil on EDM performance against various parametric levels of I_p, T_{on}, duty cycle, and V_G was illustrated by Mishra and Routara (2020). According to their findings, MRR, surface finish, surface stiffness, and aerosol emission is greatly improved by 0.86 times, 16.64%, 6.46%, and 17.33%, when comparison has been developed with a hydrocarbon-based dielectric. Singh et al. (2020) compared the results of three dielectrics (Pongamia, jatropha, and kerosene) to assess the MRR, SR, and electrode wear rate (EWR) in the course of EDM principle. They found that Pongamia dielectric had delivered better results of the responses, followed by jatropha and kerosene. Das et al. (2020) exercise EDM to inspect the MRR and SR of the Ti–6Al–4V against I (4–16 A), T_{on} (50–250 μsec), pulse off-time (T_{off}: 10–50 μsec), and V_G (20–50 V). They were nominated trans-esterified neem oil as a dielectric liquid. After contrasting the findings with the kerosene dielectric, they declared that green dielectric exhibits 17% less SR and 22% higher MRR. Basha et al. (2021) experimentally explored the role of jatropha curcas and biodiesel on MRR and EWR while EDM of Ti–6Al–4V. They were considered voltage, I, T_{off}, and T_{on} as input parameters. The results showed that 40 V, 21 A, T_{off} = 240 μsec, T_{on} = 475 μsec was the optimal setting for higher MRR. Whereas, for attaining low EWR, voltage (for biodiesel oil: 85 V and for jatropha oil: 55 V), 9 A, T_{on} = 475 μsec, and T_{off} = 168 μsec was the best combination. In another study it was reported that increase in pulse current raised the MRR magnitude (Nieslony et al., 2023).

However, finite work is available on the nanopowder mixed biodegradable dielectric to further tune the arcing, thermal stability, and corrosion resistance pertaining to vegetable mixed EDM of different alloys. For instance, MangapathiRao et al. (2021) probed the significance of alumina powder in the sunflower oil during EDM of AISI D2 steel. Three responses, i.e., MRR, SR, and TWR, were examined against multiple input factors with the aid of copper electrode. They concluded that a mixture of alumina mixed with sunflower oil improves all the output parameters. They further claimed that the emission of fumes and hazardous vapors is abolished due to the high biodegradability and notable fire point of sunflower oil than that of kerosene oil. In the same way, Bajaj et al. (2020) used Kusum oil and multiwall carbon nanotubes (MWCNT) together to optimize the variables of rotary EDM. For optimization, they were taken response surface methodology (RSM). After

relating the outcomes to traditional dielectric, the investigators anticipated that cutting rate and surface finish are upgraded by 57.14% and 54.57%, respectively. Moreover, the use of Kusum oil in the replacement of kerosene oil during the EDM process has also been suggested by the researchers owing to its novel qualities such as superior density, excellent heat conduction for good cooling conditions, low dielectric constant to avoid energy loss, high oxidative content for decreasing the harmful gases, and low carbon emission shrinks the metallurgical flaws which tend to minimize the manufacturing cost. According to Modica et al. (2011) and Leão and Pashby (2004), EDM process under powder mixed biodegradable dielectric is an effective, versatile, and reliable way to improve output variables as well as increase the sustainable machining. Therefore, the current investigation was mixed graphene nanoparticles in the RBO to achieve the objective.

From the above literature, it can be inferred that very few studies were composed on the concept of nano additive-oil blended EDM of various superalloys. However, in the EDM process, an emulsion of graphene nanoparticles and rice bran oil is not investigated yet, as far as Ti–6Al–4V is chosen as cutting material. Therefore, the primary focus of this study is to scrutinize the impact of different input parameters on the MRR, SR, and SEC by mixing graphene nanopowder in rice bran oil for sustainable production. Six input parameters, i.e., polarity, discharge current (DC), electrode type (ET), pulse time ratio (PTR), graphene concentration (G_C), and surfactant concentration (S_C), were taken in this study. Taguchi's approach (L18 orthogonal array) was elected to accomplish experimentation. The results were statistically analyzed and tested. To collect evidence, a scanning electron microscope (SEC), energy dispersive x-ray (EDX), and optical microscope were engaged. Since the EDM process is inherently stochastic, with potential non-linear and interacting relationships between input and output factors significantly impacting its performance. Modeling such complexity is challenging, necessitating the use of an artificial neural network (ANN) in this study. Therefore, this research study presents a comprehensive investigation on machining performance of graphene-based bio-dielectric along with ANN based process modelling. Furthermore, multi-objective optimization analysis is carried out to find the optimal operating conditions in order to optimize the machining responses using bio-dielectric. The proposed artificial intelligence-based modelling and optimization of the EDM process contributes to the realization of smart manufacturing and industry 4.0 vision.

2. Materials and methods

2.1. Workpiece and electrodes

In this research, Ti–6Al–4V was employed as a cutting material. The size (length × width × thickness) of the workpiece was 100 mm × 80 mm × 15 mm. The use of the said Ti material is due to its extensive applications in different industrial sectors including petrochemical, medical, automotive, military, aerospace, and engineering structures (Abu Qudeiri et al., 2018; Li et al., 2021; Tiwary et al., 2015). Table 1 summarizes the salient characteristics of Ti–6Al–4V (Ishfaq et al., 2023c; Hasçalık and Çaydaş, 2007), whereas its chemical composition was recognized by optical emission spectroscopy (see Table 2). To carry out machining, three separate electrodes, i.e., aluminium (Al), brass, and copper (Cu), were engaged, as shown in Fig. 1. The key attributes of aforementioned electrodes are provided in Table 3 (Farooq et al., 2022; Kah et al., 2015; Ahmed et al., 2019).

2.2. Experimental setup

Owing to the high strength of Ti–6Al–4V, it becomes challenging to machine it through conventional techniques. For that reason, the EDM die sinker (manufactured by Creator, Taiwan) was operated to perform experiments. The actual machining arrangements and schematic of the EDM process are portrayed in Fig. 2. Whereas Fig. 3 expresses the working chemistry of the EDM process. For experimentation, a separate container of 1500 ml capacity and with a stirrer mechanism was fabricated to make a homogenous mixture of graphene particles in the rice bran oil. The concentration of RBO in the container against each experiment was taken as 250 ml. The chief properties of RBO are summarized in Table 4. On the other side, the amount of graphene nanopowder was nominated as a variable and its three concentrations (0.3 g/L, 0.5 g/L, and 0.7 g/L) have been used during this study. It is important to mention that the above-mentioned concentrations of graphene nano-powder were taken on the basis of 1-L RBO. However, for each experimental run these quantities of nano-powders were adjusted accordingly as per the 250 ml volume of RBO for each experiment. Moreover, the selection of the three different concentrations of graphene nano-powders in the RBO were taken by consulting different published literature. Therefore, preliminary trials were conducted on the basis of various concentrations of graphene nano-powder and the selected concentrations were found to be the suitable, because if the concentration of graphene was exceeded beyond the 0.7 g/L then agglomeration phenomenon was observed, and if the graphene was used below the threshold, then no significant removal of material was found.

Graphene particles consist of carbon atoms, which are arranged like a honeycomb confirmation. These particles have Sp^2-hybridization in such a manner that one carbon atom is bonded with the rest of the three carbon atoms at a bond angle equal to 120°. Thus, they form a hexagonal framework (Heydari-Bafrooei and Ensafi, 2019). The use of particles is also very common in multiple areas, including the medical industry, dentistry, sensors devices, heat-sink equipment, and various energy storage batteries because of their exclusive features (Priyadarsini et al., 2018; Ge et al., 2018; Yang et al., 2013), as tabulated in Table 5.

It is pertinent to explain that when nano-powder is blended with the

Table 2
Elemental composition of substrate material.

Elements	Ti	Al	V	O	C	N	Fe	H
Wt. %	90.3	6.42	4.32	0.21	0.06	0.0056	0.30	0.003

Table 1
Fundamental characteristics of specimen.

Characteristic (Unit)	Value
Density (kg/m^3)	4.4×10^3
Hardness (HRC)	28–36
Elastic modulus (GPa)	113
Shear strength (MPa)	550
Thermal conductivity (W/mK)	6.7
Electrical resistivity (Ωm)	1.72×10^{-6}
Melting temperature (K)	1876–1932
Ultimate tensile strength (GPa)	0.83

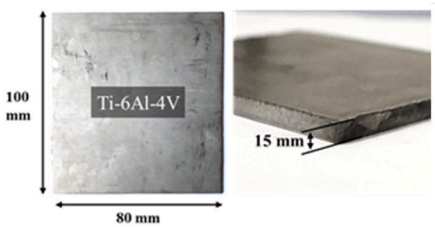

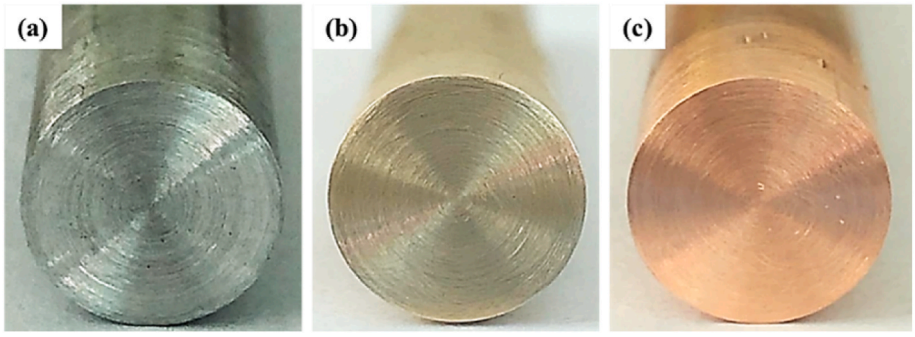

Fig. 1. Electrode materials. (a) Aluminium, (b) Brass, (c) Copper.

Table 3
Essential attributes of electrodes.

Property	Unit	Aluminium	Brass	Copper
Hardness	MPa	100	124–1030	80–85
Melting point	Kelvin	933.15	1213.15	1356.15
Density	g/cm^3	2.71	8.73	8.90
Thermal conductivity	W/mK	226	109	385
Electrical resistivity	Ωm	2.65×10^{-8}	0.9×10^{-7}	1.7×10^{-8}

dielectric fluid, then the particles may cause suspension and agglomeration in the vessel of EDM, resulting in the deterioration of surface asperities, loss of energy, and minimizing the rate of machining. The problem that persists with the powder mixed EDM can be eliminated by adding a certain concentration of surfactant. Surfactant controls the sparking gap, amplifies the conductivity, and reduces the agglomeration (Ishfaq et al., 2024). Thus, abnormal discharges can be improved by the mixing of surfactant along with the nano-powder. Fig. 4 illustrates a comparison between the EDM process with and without surfactant. The left schematic depicts the powder mixed EDM (PMEDM) process, whereas the right schematic displays the surfactant based PMEDM. The current work utilized Span 20 as a surfactant owing to its high solubility, excellent dispersion, short bridging time, and more hydrophobicity. In addition to that, three different concentrations of Span-20 (8, 10, and 12)g/liter have been used in this research against the RBO. Some of the key traits of Span 20 are provided in Table 6.

2.3. Pilot study

The six control parameters (polarity, electrode type, discharge current, pulse time ratio, graphene concentration, and surfactant concentration) were considered in the present work. The selection of previously stated factors mainly relies on two benchmarks, (i) greater impact of control variables on responses, (ii) Or the particular variable is not assessed against the responses. Other than those mentioned above, all other variables remained constant, as compiled in Table 7.

After the selection of input variables, it is essential to identify parametric levels. For that purpose, a pilot study was conducted before starting actual experiments on a sample material. During initial trials, a 0.2 mm depth of cut was applied. For cutting the workpiece, all three tools, namely aluminium, brass, and copper, were employed. These trials assist to find desired levels of all the factors. The attainment of adequate impressions was the key attention while nominating the parametric levels. Primarily, excessive burn marks, small pits, and scalds were observed on the specimen's surface due to uncontrolled discharging or arcing, as represented in Fig. 5. Hence, only those parametric levels were appointed after initial experiments, which have delivered accurately machined cavities. The elected factors and their corresponding levels are summarized in Table 8.

2.4. Machining parameters

The effectiveness of the EDM process has been gaged in respect of

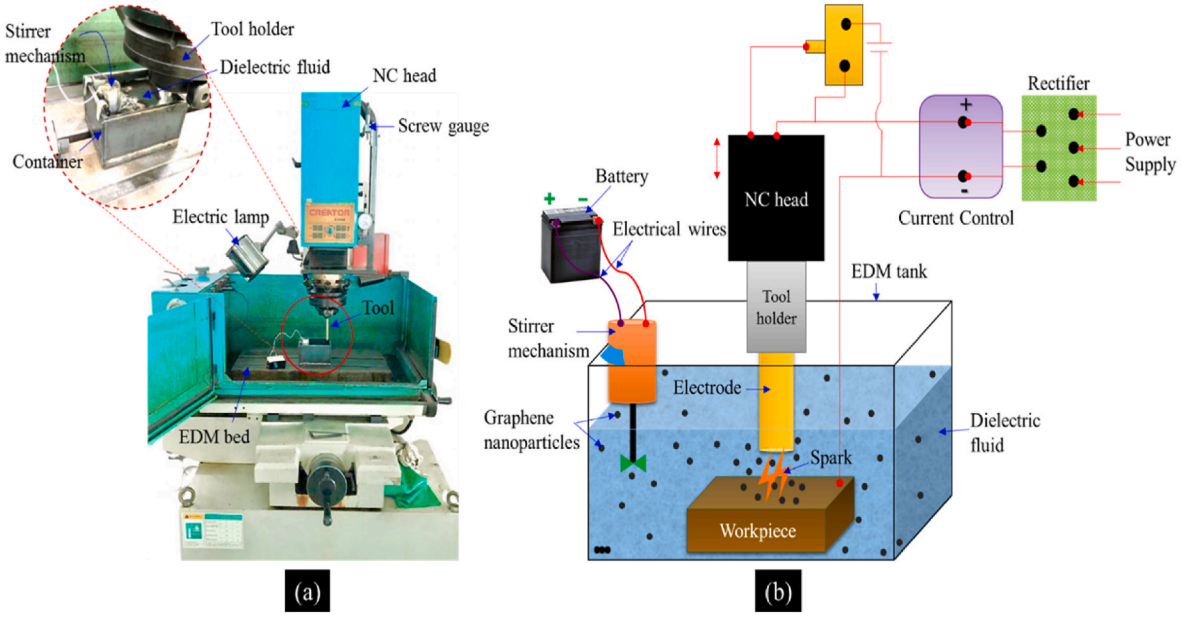

Fig. 2. EDM die sinker. (a) Actual machining setup, (b) Schematic of EDM.

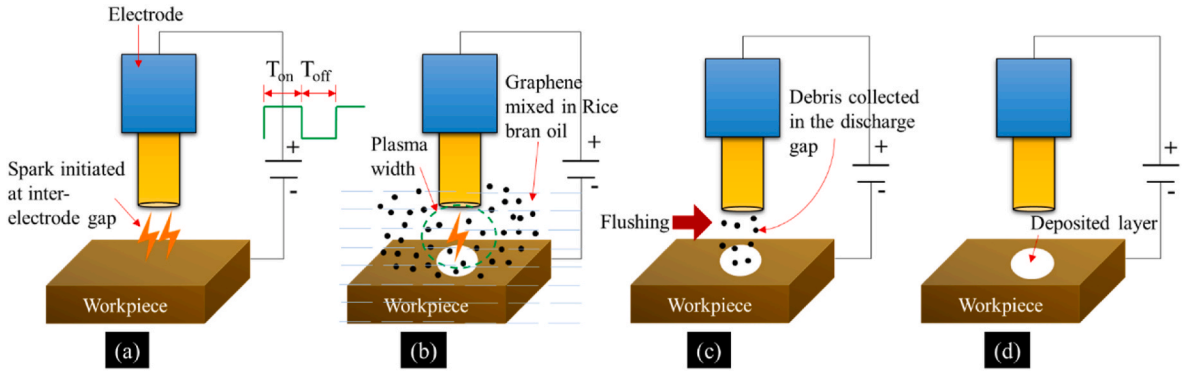

Fig. 3. Working chemistry of EDM process. (a) Tool approaches the workpiece and generates electric sparks, (b) Presence of graphene particles increase the discharge gap, (c) Formation of molten pool, (d) Cavity formation and retracting of electrode.

Table 4
Characteristics of rice bran oil.

Name (Unit)	Value
Density (g/cm^3)	0.8682
Flash point (°C)	150
Dielectric constant	2.7
Moisture content (%)	1.5
Viscosity at 40°C (centistokes)	8.92
Thermal conductivity (W/mK)	0.20

Table 5
Important traits of graphene nano-powder (Madurani et al., 2020).

Name (Unit)	Value
Colour	Grayish Black
Carbon content (%)	More than 99
Optical transparency (%)	97.7
Thermal conductivity (W/mK)	5000
Young's modulus (TPa)	0.25–1.0
Specific Surface area (m^2/g)	2630
Electrical conductivity (Siemens/m)	1738

three different responses, namely MRR, SR, and SEC. In spite of these variables, carbon dioxide (CO_2) emissions for RBO and conventional dielectric were also calculated. All these responses are equally important in the electric spark machining of Ti–6Al–4V because they define the power, cost, and effectiveness of the process. Such as, MRR symbolizes the economical factor, SR portrays the surface finish, which enhances the quality of the operation, SEC illustrates how much power is lost or saved during machining, and CO_2 emissions determines the sustainability aspect of the EDM process. Moreover, Taguchi's design of experiment (L18 orthogonal array) was nominated for experimentation. Since it has been proven as a well-justified, robust, and effective method (Shen et al., 2017), therefore it has been deliberated in the current study.

2.5. Data collection and analysis

For calculating MRR, Eq. (1) was used, whereas SEC was computed by utilizing Eqs. (2) and (3).

Table 6
Properties of span 20 (Kolli and Kumar, 2015a).

Attribute	Chemical formula	Flash point	Water content	Acid value	Density
Value	$C_{18}H_{34}O_6$	110 °C	Less than 1.5 %	4–8	1.032 g/ml

Table 7
Fixed parameters.

Parameter	Value
Pulse off-time	100 μsec
Spark voltage	5 V
Dielectric type	Rice bran oil
Dielectric quantity	250 ml (for each experiment)
Powder type	Graphene nano-powder
Surfactant type	Span 20

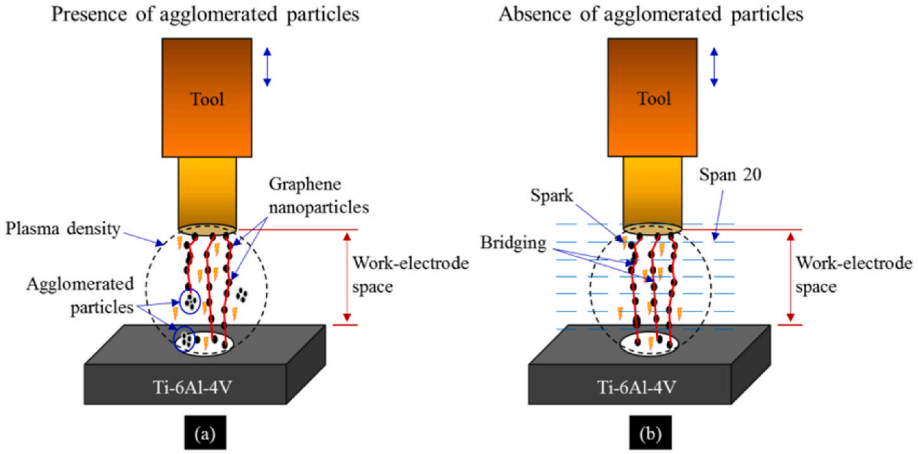

Fig. 4. PMEDM process. (a) Without surfactant, (b) With surfactant.

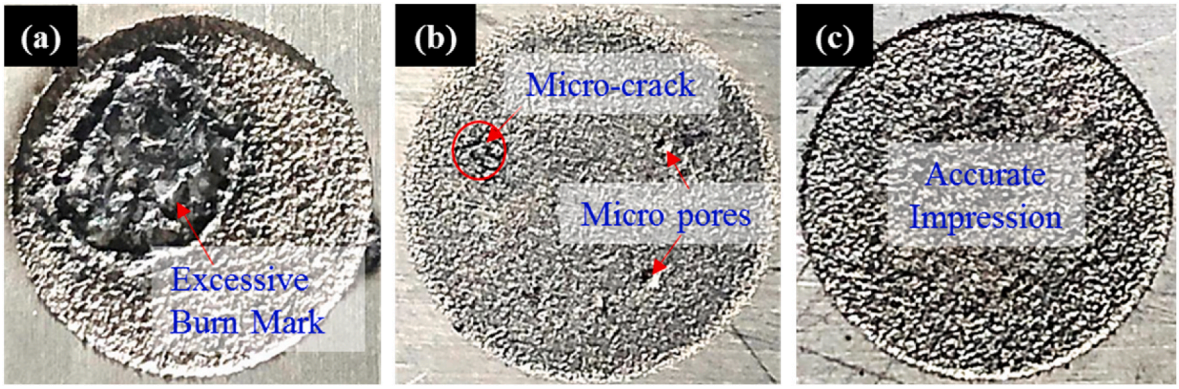

Fig. 5. Machined surfaces of preliminary trials showing. (a) Excessive burning, (b) Pit and scald, (c) An accurate impression.

Table 8
Input factors and their levels.

Factor	Unit	Parametric levels		
		1st Level	2nd Level	3rd Level
Polarity	–	Normal	Reverse	–
Electrode type	–	Aluminium	Brass	Copper
Discharge current	amperes	6	8	10
Pulse time ratio	–	0.5	1.0	1.5
Graphene concentration	gram/liter	0.3	0.5	0.7
Surfactant concentration	gram/liter	8	10	12

$$MRR\left(\frac{mg}{\min}\right)=\frac{M_B-M_A}{t} \tag{1}$$

$$E=I(\text{amperes})\times V(\text{volts})\times T_{on}(\mu\ \text{sec}) \tag{2}$$

$$SEC\left(\frac{J.\text{sec}}{mg}\right)=\frac{E}{V_m} \tag{3}$$

Where, M_B, M_A, t, E, and V_m designate the mass of cutting material before experiments, mass of workpart after experiments, machining time, consumed energy, and volume of material removed, respectively.

The SR was quantified in terms of the average roughness (R_a) value. R_a is simply defined as a mean value between the surface's crests and valleys. Against every experiment, it was assessed through an SR meter (Model: Surtronic S128 by Taylor Hobson). The cutoff and assessment length were adjusted at 0.8 mm and 4 mm, respectively. However, the complete calculation methodology for CO_2 emissions and percentage reduction of CO_2 emissions have been explained in sections 4 and 5.

After data collection, statistical analysis was accomplished to broadly investigate the influence of different six selected variables on the MRR, SEC, and SR, as long as the EDM setup is arranged using nanographene mixed RBO dielectric. The magnitudes of each output variable were noted against all the parametric levels. For example, polarity has two kinds (such as reverse or normal polarity). Out of eighteen experiments, nine were accomplished at the reverse polarity and the remaining nine at normal polarity. In the same manner, DC has three states; thus, six trials were done for all three conditions (6 A, 8 A, and 10 A). Based on this concept, other input parameters were treated. To analyze the data, main effect plots and bar charts were plotted. The main effect plots were drawn by taking the mean values of a particular response against parametric levels. For a detailed insight into the process, proof was obtained through SEM (Model: VEGA3 manufactured by TESCON), EDX, and an optical microscope. In the end, the optimal parametric combination has been put forward with the aid of NSGA-II followed by ANN model. Several solutions have been generated using NSGA-II. To obtain a single optimized solution, The Technique for Order of Preference by Similarity to Ideal Solution (TOPSIS) approach was applied. The details associated with the ANN based modelling and multi-objective optimization analysis are provided in the next section.

2.6. Artificial intelligence (AI) as a key process enhancement tool

Machining performance is greatly improved by AI through the use of sophisticated algorithms and data analytics. In the journey of leveraging AI for performance enhancement, the process begins with careful modelling for MRR, SR, and SEC. Selecting an appropriate AI model architecture, tailored to the nature of the problem, sets the foundation. The subsequent training phase involves meticulous data preparation, ensuring diversity and eliminating biases in the dataset. One important component is AI-driven process optimization, which performs large data analysis to spot trends and optimize machining parameters like cutting rates, surface finish, and energy consumption in the context of EDM for higher efficiency. In this aspect, firstly the training, testing and validation has been performed by modelling the magnitudes of response measures. It is crucial to extract meaningful information, and during training through ANN, the model adjusts its parameters to minimize the disparity between predicted and actual outcomes. However, testing of modelling data evaluates the model's generalization performance on a separate dataset, while validation encompasses hyperparameter tuning and robustness testing to enhance the model's reliability. Addressing biases is the integral aspect of the robust design phase. Finally, optimization involves streamlining the model for efficient deployment, considering factors like size, speed, and resource requirements. This systematic approach, from modelling to optimization, ensures the development of AI systems that not only excel for EDM but also demonstrate robustness. The AI based multi-objective optimization helped in evaluating the choice for the optimal parameters for input variables for getting the higher values of MRR, lower magnitudes of SR and SEC (Ishfaq et al., 2023d). Therefore, AI has a lot to offer machining, including increased productivity, better quality, predictive maintenance, and insightful data analysis that all work together to improve manufacturing performance.

2.6.1. ANN based modelling

Artificial neural network (ANN) is one amongst the versatile modelling algorithms of machine learning that can detect the hidden features and relationships among the variables present in the dataset (Shams et al., 2021). ANN can effectively approximate the nonlinear and complex function that demonstrates it as a universal function approximator (Ashraf et al., 2022). ANN can work well with various types of datasets like numerical, categorical, image, audio, time series etc., thus making it suitable for various applications. Additionally, the architecture of ANN provides parallel computational processing capabilities that enable the algorithm to efficiently process heaps of data and perform complex computations, making them well-suited for tackling challenging and computationally intensive tasks (Uddin et al., 2020).

Therefore, ANN based process models are applied for solving different problems in finance, image recognition, natural language processing, and many others (Valaskova et al., 2020). Thus, ANN algorithm is applied to build the process models for MRR, SR and SEC of the EDM process.

2.6.2. Evaluation criteria

The ANN based process models are required to be rigorously evaluated by statistical performance measures to investigate their modelling performance. For this purpose, co-efficient of determination (R^2) and root mean squared error (RMSE) are utilized for the evaluation of predictive performance of the ANN model. The mathematical expression of R^2 and RMSE is given as:

$$R^2 = 1 - \frac{\sum_{i}^{N} (y_i - \widehat{y}_i)^2}{\sum_{i}^{N} (y_i - \overline{y}_i)^2} \tag{4a}$$

$$RMSE = \sqrt{\frac{1}{N} \sum_{i=1}^{N} (\widehat{y}_i - y_i)^2} \tag{5a}$$

Here, y_i represents the true value of the output variable, whereas $\widehat{y}_i$ is the ANN based simulated response against the observations of input variables. Similarly, $\overline{y}_i$ is computed to be the mean value of y_i. R^2 is a metric used to evaluate the modelling accuracy of the ANN model. R^2 varies from 0 (indicating poor predictability) to 1 (indicating a strong functional relationship). On the other hand, the root-mean-squared error (RMSE) quantifies the deviation between the true and model-based simulated responses and is to be minimized.

2.6.3. Multi-objective optimization using genetic algorithm

The genetic algorithm is a meta-heuristic approach that is applied to estimate global solution for the optimization problem by a reasonable timeframe and computational resources (Deb, 1999). The genetic algorithm works on a population of individuals, where each individual has a mathematical representation. Initially, a random population of individuals is created, and the fitness of each individual is evaluated. In the next step, mutation and crossover operations are applied on the individuals that result in the formation of new offspring (Deb, 1999). The fitness of each offspring is evaluated, and the most favorable one is selected for creating the next generation. This iterative process of modification in the individuals continues so as to converge to the global minimum thereby optimized conditions of the input variables are estimated. The genetic algorithm is well-suited for multi-objective optimization analysis. It can handle conflicting objectives by non-dominated sorting genetic algorithm-II (NSGA-II) and evaluating individuals across multiple fitness functions, resulting in a set of Pareto optimal solutions (Deb et al., 2002). One of the most well-liked multi-objective optimization algorithms is NSGA-II, which has three unique features: a simple crowded comparison operator, a quick crowded distance estimate process, and a quick non-dominated sorting strategy. By promoting diversity and convergence, the algorithm efficiently explores trade-offs and provides decision-makers with a range of optimal solutions to choose from. This makes the genetic algorithm a valuable tool for real-world problems involving multiple objectives. Thus, in this work, the optimization problem is defined considering to maximize MRR and minimize SR and SEC and the optimal solution is obtained after solving the problem through genetic algorithm solver. The optimal solution is selected by TOPSIS method – distance based technique commonly used in literature to find the optimal solution from the Pareto front (Tariq et al., 2022).

3. Results and discussion

The present research utilized Taguchi's orthogonal structure (L18) to manage experiments on EDM setup, when a mixture of graphene nanoparticles and the RBO is made for making impressions over the surface of Ti–6Al–4V. After experimentation, the findings were carefully compiled, as mentioned in Table 9. The machined cuts obtained against each experiment are shown in Fig. 6. Through statistical plots, the effect of each response was individually examined against all six input parameters, as depicted in the approaching sections.

3.1. Influence of input variables on material removal rate

3.1.1. Effect of type of polarity

First, the impact of change in the polarity of EDM is discussed on MRR. Polarity has two states: normal polarity and reverse polarity. Normal polarity means that the electrode is negatively charged, and the workpiece holds positive charges. Contrary to that, vice versa is tolerable for reverse EDM. Fig. 7 shows the role of both EDM polarities on the MRR using nanographene-mixed biodegradable dielectric. It can be noticed that the wearing of material from the work cavity is notably higher at the normal polarity of the EDM. It has been illustrated that, when normal polarity is used, significant energy is delivered to the machined cavity rather than the electrode, which eat away more material from the workpart and results in the formation of deep craters (Khan and Hameedullah, 2011), and eventually, MRR is increased. On the other side, reverse polarity has yielded less MRR. Whenever the polarity of EDM is reversed, the flow of electrons is also altered. In this way, the large amount of material starts melting and vaporizing from the electrode in comparison to the workpiece. Thereof, the minimum value of MRR is observed at reverse EDM polarity. Fig. 8(a and b) depicts the craters' size on the cut cavity at two kinds of EDM polarity. Hence, cutting Ti–6Al–4V via the EDM process at normal polarity is desirable over reverse polarity as far as MRR is studied.

3.1.2. Effect of electrode type

The effect of aluminium, brass, and copper on MRR during EDM of Ti–6Al–4V under graphene mixed RBO is portrayed in Fig. 7. Amongst the three electrodes, brass is the one which has provided outstanding results of MRR owing to its lowest thermal conductivity (109 W/mK). This does not permit the brass to engross much heat energy, and maximum energy delivers to the workpiece during the material erosion process. As a result, the rate of material erosion becomes higher (Khan, 2008). The highest value of MRR (58.58 mg/min) due to brass electrode is linked with the parametric settings involved during experimentation against both the trials i.e. 5th and 6th. In 6th experimental trial the combination of parameters used includes highest value of discharge current (10 A) and pulse time ratio PTR (1.5) along with the least concentration of graphene powder (0.3 g/L). This optimal/unique set of parameters provides relatively adequate discharge energy in the cutting regime in comparison to the rest of the settings. The availability of sufficiently high amount of discharge energy in the workpiece-electrode gap induces an intense heat flux into the target surface. This causes a greater amount of material to be removed from the workpiece as result of comparatively intense melting and evaporation. It is pertinent to mention that not only significant amount of workpiece material eroded due to electro-erosion phenomenon on this particular setting rather this combination also facilitates the proper evacuation of the melted debris. Thus, the chance of melt-redeposit reducing which help to decrease the machined surface asperities as well. As the eroded material cannot rejoined with the machined profile therefore MRR value gets improved/enhanced because it is linked with the amount of material removed from the workpiece surface. Moreover, due to the non-magnetic effect of brass, the nano-graphene in the dielectric, when charged while discharging, did not stick with the electrode's surface. Consequently, smooth sparking takes place, which tends to give high MRR. The same reason has also been narrated by Ishfaq et al. (2020). Oppositely, in the case of the copper electrode, MRR is enormously reduced. Though graphene nanoparticles are available in the dielectric fluid, which gets

Table 9
DOE and responses' magnitudes.

Exp. No.	Polarity	ET	DC (A)	PTR	G_C (g/liter)	S_C (g/liter)	MRR (mg/min)	SR (μm)	SEC (J.sec/mg)
1	Normal	Al	6	0.5	0.3	8	0.17	2.89	0.53
2	Normal	Al	8	1.0	0.5	10	0.78	3.5	0.31
3	Normal	Al	10	1.5	0.7	12	1.44	2.9	0.31
4	Normal	Brass	6	0.5	0.5	10	1.10	5.67	0.08
5	Normal	Brass	8	1.0	0.7	12	7.32	6.17	0.03
6	Normal	Brass	10	1.5	0.3	8	58.58	8.73	0.01
7	Normal	Cu	6	1.0	0.3	12	0.62	5.87	0.29
8	Normal	Cu	8	1.5	0.5	8	1.73	7.53	0.21
9	Normal	Cu	10	0.5	0.7	10	1.49	6.7	0.10
10	Reverse	Al	6	1.5	0.7	10	0.25	6.5	1.08
11	Reverse	Al	8	0.5	0.3	12	0.41	5	0.29
12	Reverse	Al	10	1.0	0.5	8	1.34	9.07	0.22
13	Reverse	Brass	6	1.0	0.7	8	0.13	5.43	1.38
14	Reverse	Brass	8	1.5	0.3	10	0.53	9.37	0.68
15	Reverse	Brass	10	0.5	0.5	12	2.02	6.7	0.07
16	Reverse	Cu	6	1.5	0.5	12	0.80	8	0.34
17	Reverse	Cu	8	0.5	0.7	8	0.82	5.8	0.15
18	Reverse	Cu	10	1.0	0.3	10	1.97	8.17	0.15

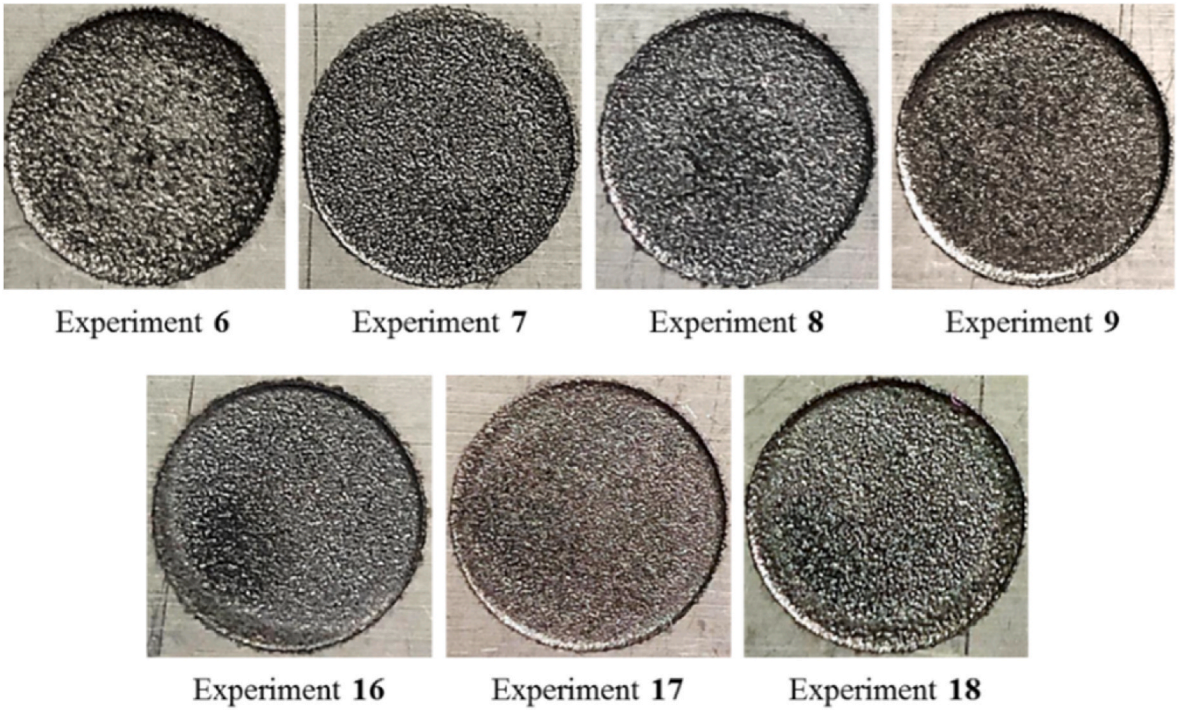

Fig. 6. Images of selected experimental cuts achieved after EDM of Ti–6Al–4V.

charged while sparking, thus a pool of ions is created. Such a large number of ions develop a guard in front of discharges. Due to this reason, a low value of MRR is realized with the Cu-electrode, followed by the brass. For the aluminium tool, the MRR is found to be lowered than that of other electrodes. The low melting temperature (933.15 K) of the Al-tool is the prime reason behind this change. During the machining of the substrate material, aluminium starts eroding more rapidly, as compared to the Ti–6Al–4V, whose melting point (1933.15 K) is extremely higher. The SEM images of the cut profiles were also collected against three tool materials, as evidenced in Fig. 10. According to these images, Al and Cu have resulted micro-cracks along with the shallow craters on the specimen's surface, as displayed in Fig. 10**(a)** and **(c)**. Whereas, in the case of brass (see Fig. 10**(b)**), material re-solidification takes place due to the absence of arcing while forming plasma columns in the work-electrode zone. Hence, to get appreciable MRR brass is a suitable candidate for the machining of Ti-alloy via the EDM process when graphene nanoparticles are mixed with the rice bran oil. The microscopic images of all the electrodes later the EDM process are shown in Fig. 9(a, b, c). This microstructural analysis indicates the different nature of craters produced on the surfaces of electrodes. Where deep craters have been observed on the surface Al electrode, while the shallow and small craters have been indicated on the surface brass and Cu electrodes.

3.1.3. Effect of discharge current

As far as Ti–6Al–4V is operated on EDM under a mixture of nano-graphene and RBO, the impact of DC on MRR is also discussed herein (see Fig. 7). The findings can be revealed that when the DC rises in the range of 6–10 A, the MRR also upsurges. The literature witnessed that discrete powerful discharges occur at a high current density which penetrates through a liquid puddle to the work cavity. This causes high melting of material from the specimen, leaving behind large and deep craters (Ni et al., 2021). The potentiality of graphene nanoparticles in the RBO also plays a role in enhancing the MRR. These nanoparticles

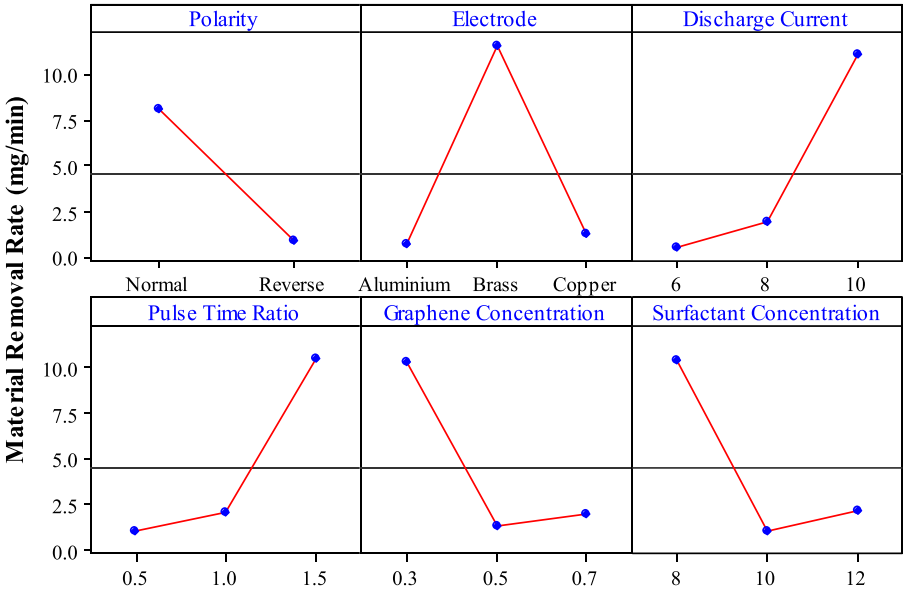

Fig. 7. Main effect plot for MRR against input parameters.

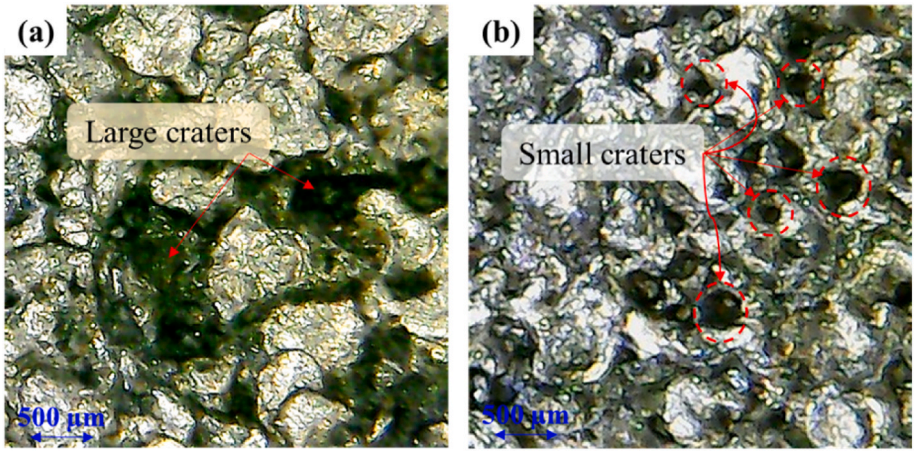

Fig. 8. Micrographs depict the craters on the Ti–6Al–4V. (a) Normal polarity, (b) Reverse polarity.

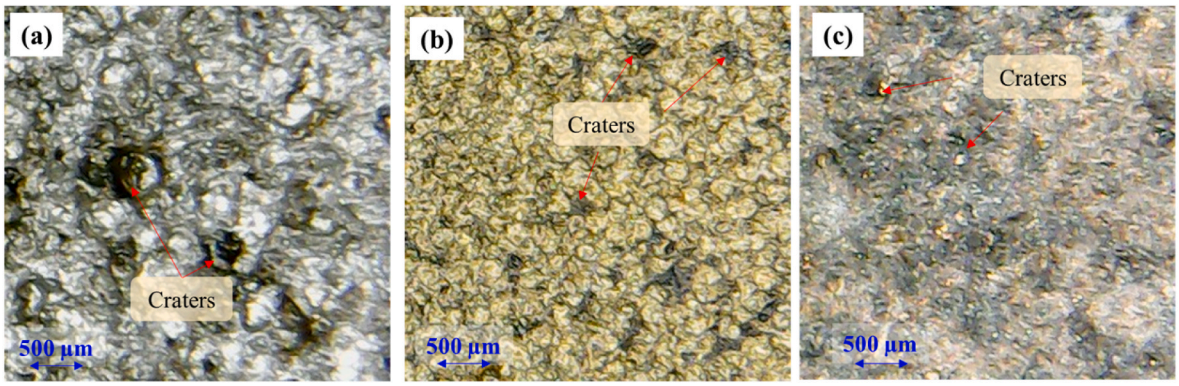

Fig. 9. Micrographs depict the craters on the electrode surface using (a) Al electrode, (b) brass electrode, (c) Cu electrode.

control the plasma gap and build bridges of charged particles from the tool to the specimen by lowering the breakdown voltages. As an effect, stable sparks are generated that correspond to multiply the MRR (Joshi and Joshi, 2019a). A comparison of craters' sizes at 6 A and 10 A is displayed in Fig. 11. Hence, it is revealed that a higher condition of DC is well-suited for attaining a higher magnitude of MRR as far as nano-graphene mixed EDM of Ti–6Al–4V is bothered.

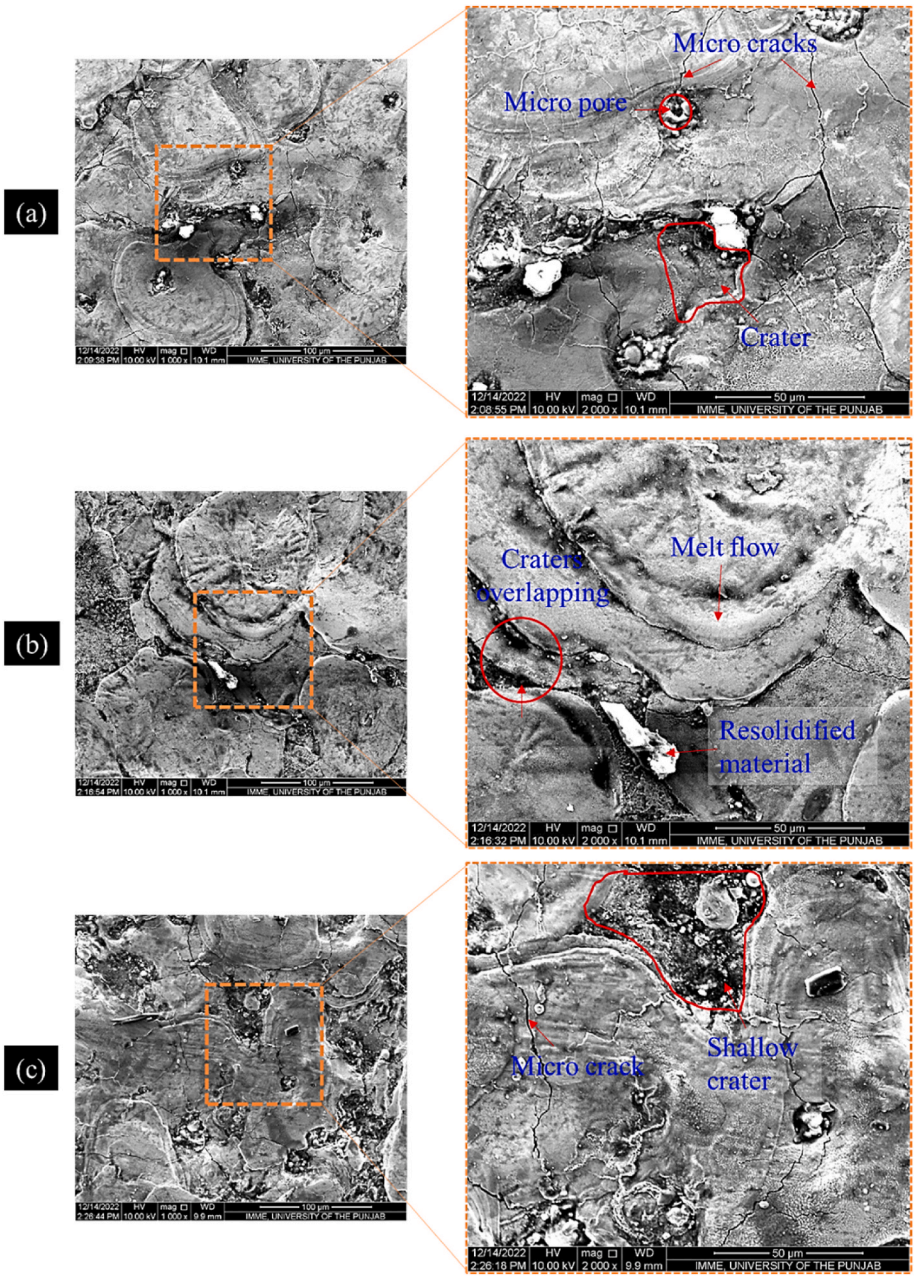

Fig. 10. SEM images portray surface texture of the machined cavities against distinct electrodes. (a) Al, (b) brass, (c) Cu.

3.1.4. *Effect of pulse time ratio*

The ratio between T_{on} and T_{off} is known as the pulse time ratio. Since T_{off} was fixed during machining, thus the value of MRR only depends on T_{on}. It is pertinent to note that the trend of PTR has appeared to be the same as for the DC against the MRR, as depicted in Fig. 7. The MRR increases with the change in PTR from lower (0.5) to a higher value (1.5) or escalates with the increase in T_{on}. This is attributed to longer pulse energy at higher T_{on}. Literature also evidenced that, at a large value of T_{on}, discharge heat is created for a longer duration in the cutting regime (Praveen et al., 2018; Moudood et al., 2015). As a result, high intensity sparks is liberated, which leads to the wear of greater material from the workpiece, resulting in the formation of deep craters. Besides, graphene particles influence the cutting process and augment the MRR by supporting/intensifying the discharge column during recurring sparking. The nanoparticles also reduce the arcing effect that may take place at a higher pulse duration. Thus, the authors claim that EDM of elected Ti material under graphene nanoparticles improve the machining characteristics due to its exclusive nature and notable impact on the discharge density within the plasma gap. The surface morphologies obtained at three levels of PTR are specified in Fig. 12. To get maximum MRR under a slurry of graphene nanoparticles and RBO, the optimum condition of PTR is 1.5.

3.1.5. *Effect of graphene concentration*

The MRR is also evaluated against the powder's concentration in the electro-spark process of Ti–6Al–4V using nanographene mixed green dielectric, as portrayed in Fig. 7. It can be detected that a lower concentration (0.3 g/L) of powder yielded high MRR. This mainly happened due to negligible suspension and agglomeration of nanoparticles in the dielectric regime, which promotes focus/control discharges between the work-electrode gaps. As a result, a remarkable value of MRR is attained when 0.3 g/L powder concentration is used. However, the opposite case is noticed with MRR when more nanopowder is added (up to 0.5 g/L) into the dielectric medium. The value of MRR is compromised at the said

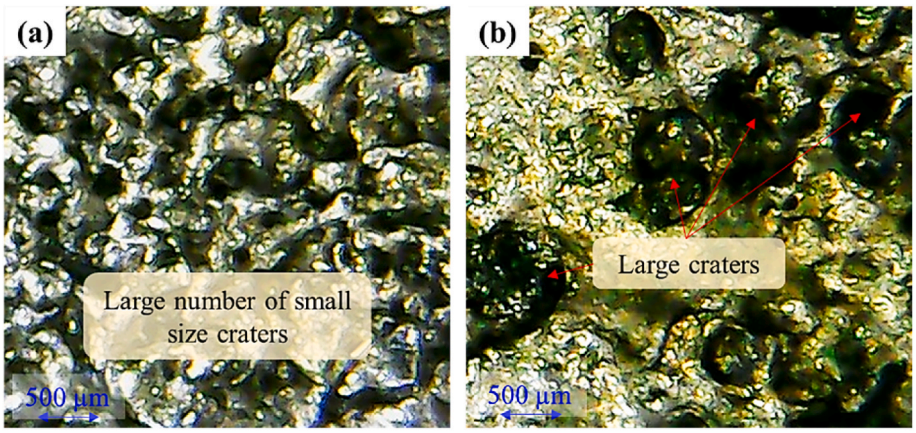

Fig. 11. Comparison of craters' size at different settings of DC. (a) 6 A, (b) 10 A.

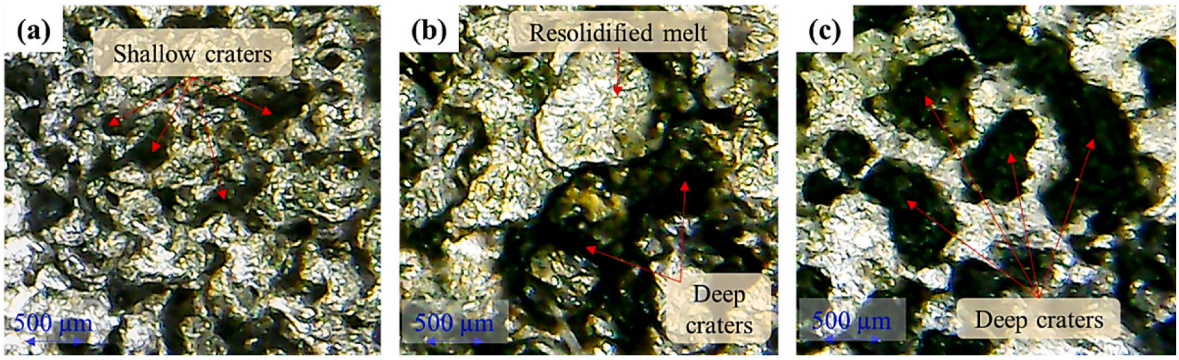

Fig. 12. Micro-texture noticed against three states of PTR. (a) 0.5, (b) 1.0, (c) 1.5.

setting because the graphene/carbon particles get deposited around the machined cavity and develop clusters which warrant the discharges do not disperse appropriately. As a result, arcing frequency is amplified instead of creating stable spark energy (Prihandana et al., 2020). EDX evidence also confirmed the presence of carbon particles on the workpiece (see Fig. 13). It is noteworthy to observe that further increase in the amount of powder from 0.5 g/L to 0.7 g/L in the dielectric liquid, MRR is marginally promoted. As per the literature, the said trend occurs due to the proliferation of discharges. Furthermore, the presence of graphene nanoparticles at a certain amount performs twice. It not only maintains the plasma gap but also develops connected chains in the space of tool and workpiece, as portrayed in Fig. 14, but also strengthens the electric sparks over the workpiece by lowering the breakdown voltages (Joshi and Joshi, 2019b). Paswan et al. (2021) declared that, at higher graphene concentration, short circuits increases due to the formation of bridges between the region of specimen and tool. As a result,

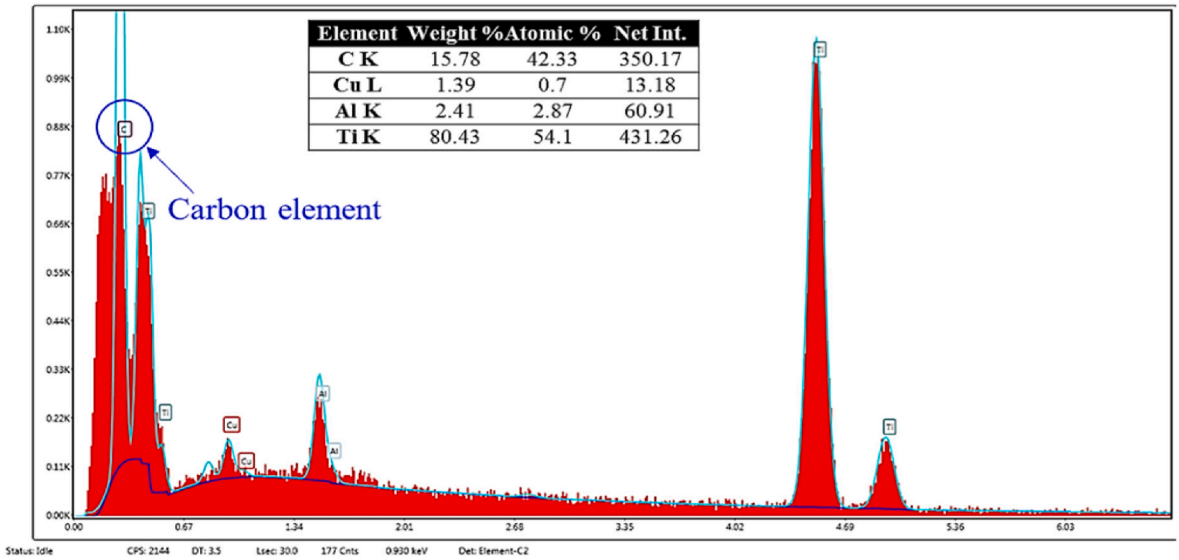

Fig. 13. EDX image shows the elemental percentage of a machined sample.

erosive discharges are prevented. The formation of bridges between the two materials because of the application of graphene nanoparticles is also displayed in Fig. 15. Amongst different concentrations of nano-powder, 0.3 g/L is highly recommended to accomplish high magnitude of MRR while sustainable EDM of Ti–6Al–4V.

3.1.6. Effect of surfactant concentration

The influence of S_C on MRR is also provided in Fig. 7. Interestingly, a similar trend is achieved, as discussed for the former parameter. The MRR initially drops with the rise in the content of Span-20 and then increases with the further addition of surfactant. Since the viscosity of rice bran oil is already higher, such as 8.2 cSt, however the addition of surfactant (10 g/L) also amplifies its viscosity. Thus, the detached particles while machining does not leave the machined region completely and make the re-deposited layer over the workpiece again (Kolli and Kumar, 2015a). Moreover, literature evidenced that factors like van der Waals forces, intramolecular forces, and surface properties may also drop the value of MRR (Feng and Hays, 2003). Contrarily, it is known that the rate of material erosion is somewhat enhanced when S_C changes from 10 g/L to 12 g/L. The higher concentration of surfactant increases the conductivity, dissolution, dispersion, and surface tension of the nanoparticles in the dielectric liquid, which augments the MRR (Kolli and Kumar, 2015a). Besides the said advantages, the agglomeration of nanoparticles is also retarded due to the existence of stereo-barriers (Wu et al., 2005). As an effect, particles are well-distributed in the dielectric liquid, which tends to enrich MRR. However, the use of a minimum concentration (8 g/L) of surfactant gives considerable results of MRR followed by 12 g/L and 10 g/L.

In a nutshell, the optimum parametric setting for getting a high value of material removal rate against the brass electrode at normal polarity is DC = 10 A, PTR = 1.5, G_C = 0.3 g/L, and S_C = 8 g/L.

3.2. Influence of input variables on surface roughness

SR is a fundamental indicator and index to surface texture. SR performs an integral part in determining how a product/component will interact with the atmosphere. It is also a perfect candidate for defining the performance of typical mechanical objects. Keeping in view the significance of SR, it is considered in the present investigation. Amongst its various parameters, only R_a is studied against the selected variables. Generally, the minimum value of R_a is taken as good for an excellent surface finish. The parametric plots of each input variable versus SR are expressed in Fig. 16.

3.2.1. Effect of type of polarity

Primarily, the surface roughness is evaluated against two polarities (normal and reverse) of EDM for machining Ti–6Al–4V using graphene nanoparticles in the rice bran oil. Fig. 16 presents the main effect plots of polarity versus SR. It is shown that normal polarity (tool = -ve and workpiece = +ve) is better for obtaining a good surface finish, followed by the reverse polarity of EDM. At normal polarity, the rate of heat dissipation is larger towards the machined cavity as compared to the electrode. During the discharging process, a small number of ions impinge on the electrode rather than on the workpart because negatively charged ions normally react with the anode at the normal state of EDM. Thus, a smooth surface (or minimum SR) is obtained when using the normal polarity of EDM. Contrarily, reverse EDM is not optimistic for a good surface finish. This is because of insufficient ionization of the graphene particles and re-solidification of melted material on the workpiece due to excessive erosion from the tool instead of the workpiece. Therefore, SR is reduced. The rise in SR at the reverse polarity of EDM is credited to the generation of deep and large craters that are portrayed in Fig. 17.

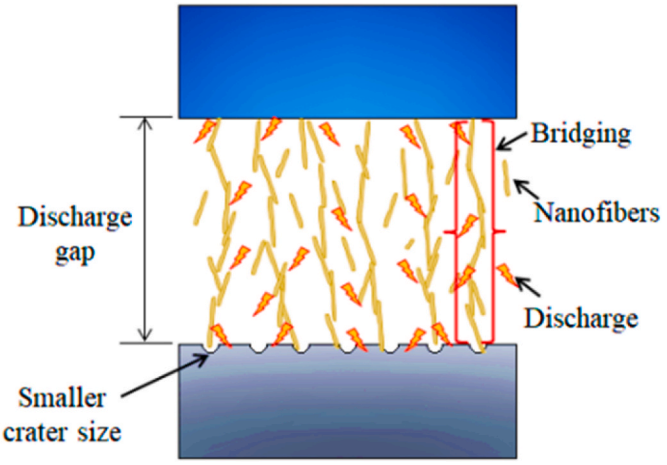

Fig. 15. Bridging effects during graphene mixed EDM (Prihandana et al., 2020).

3.2.2. Effect of electrode type

The influence of electrode type can never be ignored while EDM of Ti–6Al–4V when graphene nanoparticles are blended in the dielectric fluid. The parametric trend of electrode type versus SR is depicted in Fig. 16. It can be examined that aluminium is the only one which gives the lowest SR. The low melting point of aluminium (933.15 K) in comparison to brass (1213.15 K) and copper (1356.15 K) is the key reason behind this trend. Due to the low melting point, severe burning

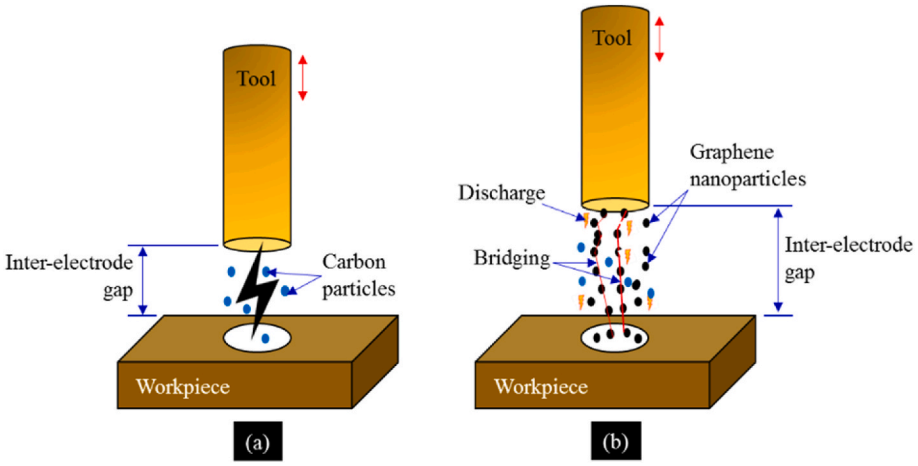

Fig. 14. Chemistry of nano-additives during EDM. (a) Kerosene-based EDM, (b) Graphene nanopowder based EDM.

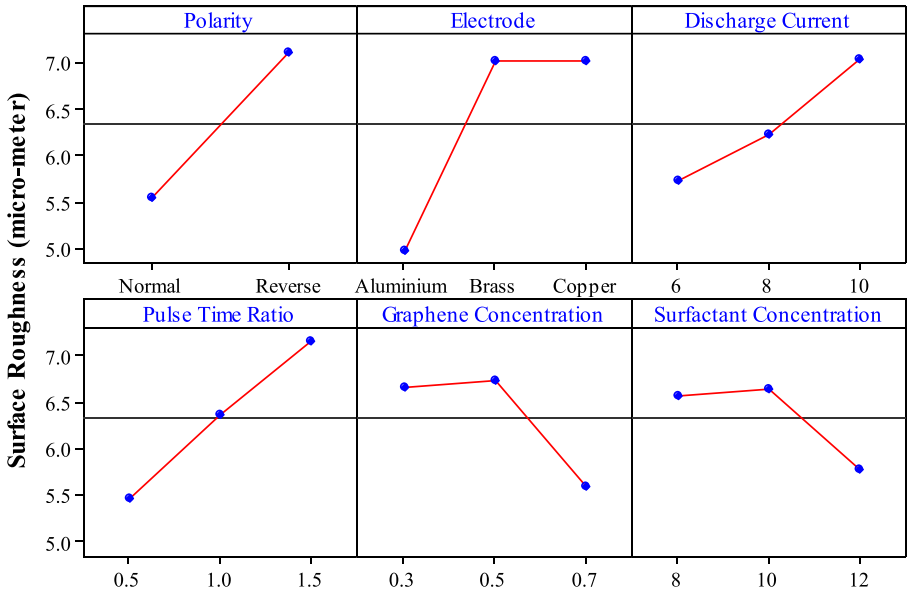

Fig. 16. Main effect plot for SR against input parameters.

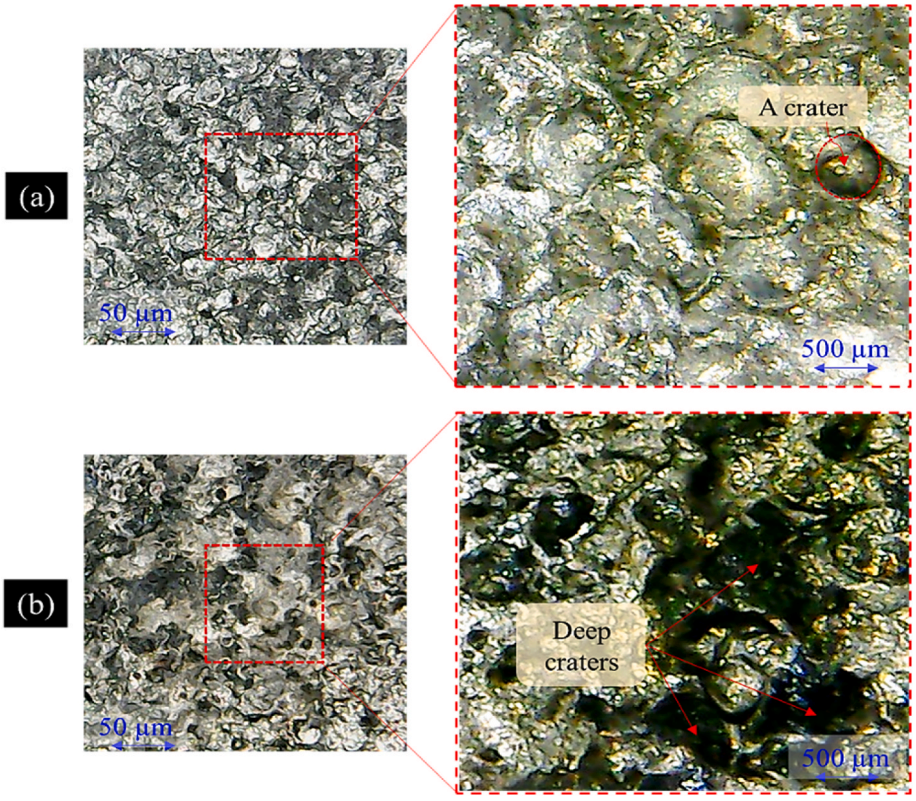

Fig. 17. Micrographs represent the surface morphology on Ti–6Al–4V at different EDM polarities. (a) Normal polarity, (b) Reverse polarity.

happens on the aluminium's surface rather than the workpart. Thus, large material is chipped out from the electrode and developed uniform texture on the operated cavity, as shown in Fig. 18**(a)**. It is pertinent to note that, for the brass and copper electrodes, no substantial change in the magnitude of SR is noticed. In another sense, both the said electrodes have provided similar outcomes in terms of surface roughness. The reason behind the brass electrode for providing inferior surface quality is due to its low heat conduction, followed by copper and aluminium, as evidenced in Table 3. In the presence of graphene additives, sparks disperse in the plasma gap containing plenty of heat, causing uneven impressions with large number of craters on the machined area, as displayed in Fig. 18**(b)**. Whereas Fig. 18**(c)** shows finite but shallow craters on the substrate surface. The roughness patterns of the machined cavities with reference to each electrode are also provided in Fig. 18. For the aluminium electrode, peak-to-valley height is lesser than that of brass and copper. Hence, the surface finish is affected by the brass and copper electrodes. It has been argued that minimum SR is found when an aluminium tool is engaged while EDM of utilized specimen under nano-

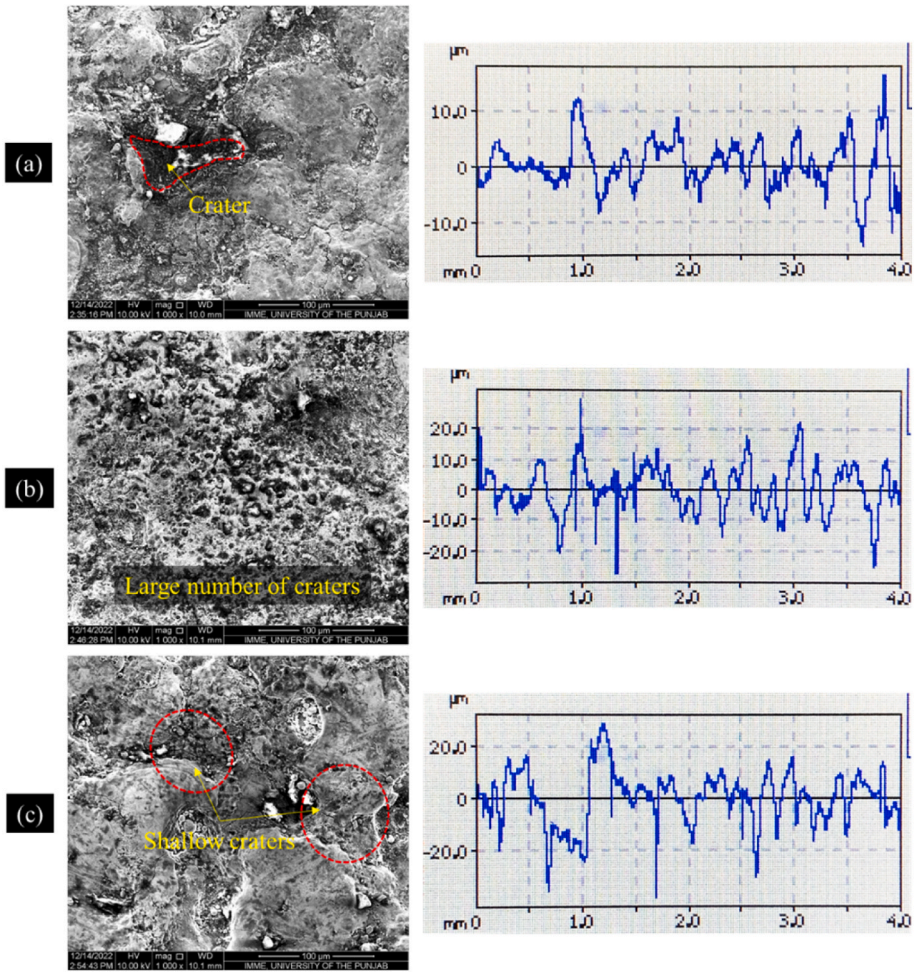

Fig. 18. Surface topology of machined cuts along with the roughness patterns for various electrodes. (a) Al, (b) Brass, (c) Cu.

graphene and RBO suspension.

As far as cutting of Ti–6Al–4V is concerned through the EDM setup, the good surface texture has been delivered by the aluminium tool. The surface morphologies of the machined impressions are already presented in the previous figure. Besides, EDX plots have also been gathered against the elected tool materials and shown in Fig. 19. According to Fig. 19**(a)**, a high percentage of Ti is noted on the cut surface as compared with other elements. Whereas, for Fig. 19**(b)** and **(c)**, the EDX images highlight the maximum percentage of Cu element on the machined periphery. This is because of the magnetic property of copper electrode. While operating the said electrode to machine Ti–6Al–4V, more carbon contents are deposited with the tool surface instead of being attached to the workpiece.

3.2.3. *Effect of discharge current*

The surface finish of Ti–6Al–4V is also altered by changing the DC when graphene particles are mixed with the RBO during the EDM process. Fig. 16 represents the main effect plot of DC versus SR. It can be foreseen that SR upsurges by the increase of DC from 6 A to 10 A. As DC increases, spark strength multiplies due to large thermal energy created within the plasma column, which accordingly yields deep and intense craters on the workpiece (Azhiri et al., 2020). Eventually, SR is raised. Thus, the minimum value of DC is more suited to get excellent surface quality on the Ti–6Al–4V considering EDM process under graphene mixed RBO dielectric. The influence of PTR on SR is also displayed in Fig. 16.

3.2.4. *Effect of pulse time ratio*

It can be predicted that surface finish diminishes by the increase of PTR or T_{on}, keeping the T_{off} fixed. The linear trend obtained in this case is due to the production of larger discharge energy in the plasma zone. Moreover, the spark is formed for a longer duration, which warrants significant melting of material from the workpart, leaving behind large and deep size craters (Goyal et al., 2018). A comparison of surface topology achieved on the workpiece during EDM process at three settings of PTR is provided in Fig. 20. Thus, SR is notably enhanced.

3.2.5. *Effect of graphene concentration*

The impact of powder concentration on the surface quality of Ti–6Al–4V is also studied in Fig. 16. It can be foreseen that G_C (0.7 g/L) is the most optimal value to attain appreciable surface finish while considering the EDM setup. Generally, for the nano-graphene mixed dielectric, gap distance increases which tend to reduce the impulsive force in the discharge region, resulting in the appearance of smoother craters (Peças and Henriques, 2008). In further addition, increase in G_C, the plasma column is fragmented into several small patches, develops bridging from tool to workpiece, and scatters heat energy more consistently, as demonstrated in Fig. 14 (Khan et al., 2015). Thus, a better surface is found at a higher concentration (0.7 g/L) of graphene. Oppositely, lower powder concentrations, such as 0.3 g/L and 0.5 g/L, have delivered a large magnitude of SR in comparison to the value obtained at 0.7 g/L. However, from a comparison point of view, SR is somewhat larger at 0.5 g/L than that at 0.3 g/L. The reason behind this is the instability of electric arcs that cause the material to erode rapidly. Nonetheless, both lower conditions (0.3 g/L and 0.5 g/L) of G_C are not

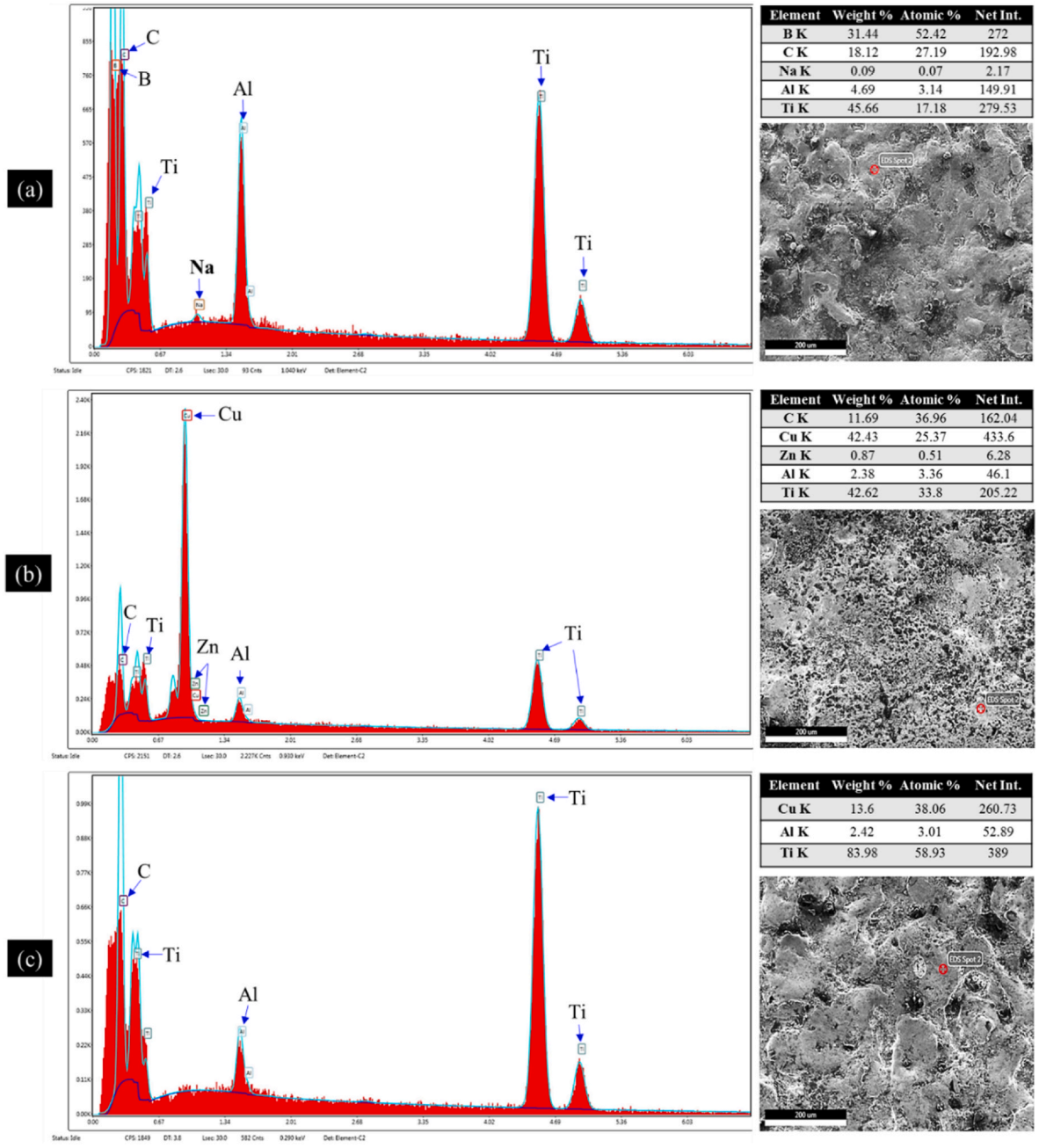

Element	Weight %	Atomic %	Net Int.
B K	31.44	52.42	272
C K	18.12	27.19	192.98
Na K	0.09	0.07	2.17
Al K	4.69	3.14	149.91
Ti K	45.66	17.18	279.53

Element	Weight %	Atomic %	Net Int.
C K	11.69	36.96	162.04
Cu K	42.43	25.37	433.6
Zn K	0.87	0.51	6.28
Al K	2.38	3.36	46.1
Ti K	42.62	33.8	205.22

Element	Weight %	Atomic %	Net Int.
Cu K	13.6	38.06	260.73
Al K	2.42	3.01	52.89
Ti K	83.98	58.93	389

Fig. 19. EDX plots against three tool materials. (a) Al, (b) brass, (c) Cu.

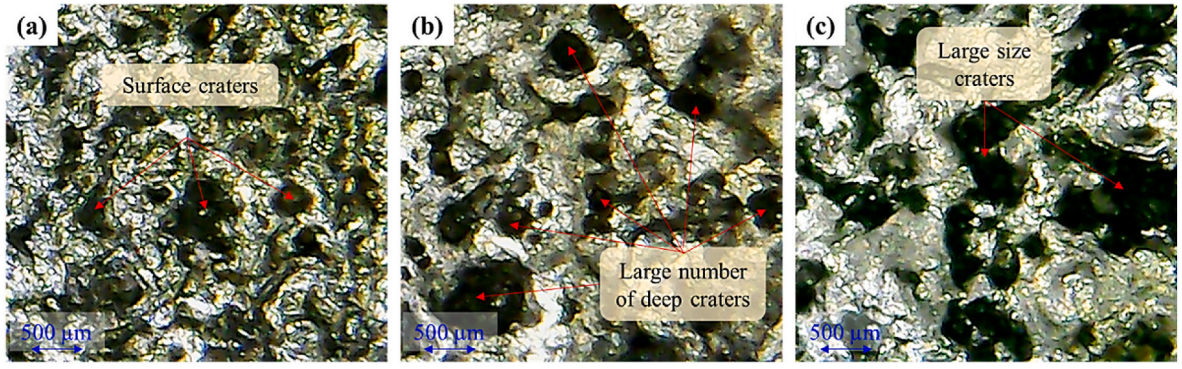

Fig. 20. Surface topology of cuts during EDM of Ti-alloy at different PTR. (a) 0.5, (b) 1.0, (c) 1.5.

favorable to use during EDM of Ti-alloy, as far as SR is studied.

3.2.6. Effect of surfactant concentrations

To study the effect of S_C on the SR, the main effect plot is developed, as shown in Fig. 16. The same trend, as discussed in the previous case, is observed for surfactant concentration. Likewise, powder concentration, the high surfactant concentration is also suitable for achieving a good surface finish on the workpiece via the EDM process. When the amount of surfactant is raised from 8 to 10 g/L, SR increases which is mainly due to increase in the dielectric conductivity, triggering the discharge energy to be more penetrated (Kolli and Adepu, 2016). However, with the further increase of S_C from 10 g/L to 12 g/L, SR is substantially improved. At very high concentration of surfactant, the agglomeration and suspension of graphene particles around the machined cavity are reduced. As an effect, the flow of debris becomes easier. Thus, SR is greatly decreased. A graphical comparison of R_a is also made using smallest and mean values against the three concentrations of surfactant (See Fig. 21).

In summary, the optimum parametric combination for getting lower SR during EDM of Ti–6Al–4V under nano-graphene blended RBO is normal polarity, Al-electrode, DC = 6 A, PTR = 0.5, G_c = 0.7 g/L, and S_c = 12 g/L.

3.3. Influence of input variables on specific energy consumption

Another chunk of the sustainable EDM process is specific energy consumption (SEC). Many products during manufacturing consume energy/resources, which straightway affects the efficiency of the system. For that purpose, it is important to study how much energy consumes by a system while machining so that losses can be minimized. Therefore, SEC is discussed herein against the six parameters while tolerating Ti–6Al–4V in the operation of EDM when nanoparticles of graphene are available in the RBO (See Fig. 22).

3.3.1. Effect of type of polarity

The effect of normal and reverse polarity on SEC is portrayed in Fig. 22. It can be predicted that normal polarity yields a lower value of SEC than reverse polarity. The reason is attributed to the MRR. Though SEC is inversely proportional to the MRR and at normal polarity rate of material melting is greater from the workpiece rather than the electrode. Therefore, SEC is decreased. Whereas the opposite case is noticed when reverse polarity is used in the electric discharge process of Ti–6Al–4V.

3.3.2. Effect of electrode type

As stated previously, Al, brass, and Cu were treated for cutting the Ti–6Al–4V. Their impact on SEC is presented in Fig. 22. It can be witnessed that Cu-electrode yields minimum SEC in comparison to other tools when nanoparticles are available in dielectric regime. The rationale behind the said case is attributed to high thermal conductivity (398.0 W/mK) of copper material than that of brass (109.0 W/mK) and aluminium (227.0 W/mK). Due to this fact, momentous heat energy is passed through the Cu-electrode, producing greater flow of current, and generating intense discharge energy in the plasma channel. Thereby, MRR is raised. Furthermore, graphene particles are also ionized because of sparking, which stabilizes the thermal energy by dispersing the discharges and increasing the spark distance, thus providing high MRR. Taking factors other than MRR invariable, SEC is inversely related to MRR. As MRR is higher for Cu-electrode, its value of SEC is accordingly smaller. Oppositely, Al-electrode is not performed well in terms of SEC owing to a protective layer of oxygen on it. This layer causes resistance in front of discharge energy; thus, energy efficiency goes down when Al is used as electrode material while EDM of Ti–6Al–4V. Brass electrode has shown intermediate response but still not efficient to give minimum magnitude of SEC under nano-additives mixed dielectric. The micrographs of the workpiece surface versus three electrodes are indicated in Fig. 23. Furthermore, the outcomes of all the electrodes were also contrasted, as represented in Fig. 24, in terms of SEC as far as EDM of selected alloy is concerned under nanographene mixed dielectric. The SEC results for copper are satisfactory, compared to the rest of the tool materials, when dielectric liquid contains graphene nanoparticles. Fig. 24 indicates a comparison of SEC versus three electrodes by using mean values of parametric levels.

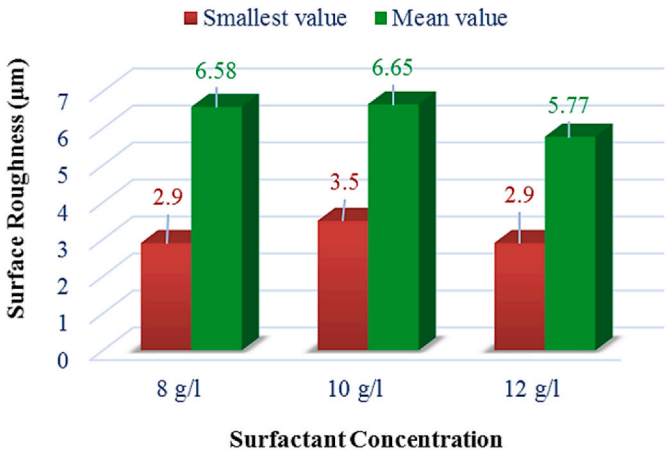

Fig. 21. A graphical comparison between SR versus surfactant concentration for the EDM of Ti–6Al–4V.

3.3.3. Effect of discharge current

The parametric trend of DC versus SEC is also displayed in Fig. 22. A decreasing curve is obtained when DC changes from 6 A to 10 A. It indicates that SEC decreases with the increase of DC as far as EDM of Ti-alloy is considered under graphene mixed RBO. At higher DC, the intensity of discharge energy is notably enriched and increases the material erosion rate. Besides, graphene nanoparticles also support the plasma column by adjusting the distance between electrode and workpart. Consequently, MRR is greatly amplified. Thereof, SEC is diminished. Hence, 10 A is the best option for attaining a minimum magnitude of SEC for the EDM of Ti-alloy when graphene nanoparticles are mixed with the green dielectric.

3.3.4. Effect of pulse time ratio

PTR is another factor that has an effect on SEC under graphene based EDM process. As said earlier, T_{off} was taken as constant parameter. Since, PTR is only belonging to pulse duration. As per the given relationship in Eq. (2), SEC is directly proportional to T_{on}. It means that increase in T_{on} also raises the SEC magnitude and vice versa. The same fact is observed herein, for the nanographene mixed dielectric in EDM of Ti material, as highlighted in Fig. 22. By increasing the T_{on} from 25 µsec to 75 µsec, keeping T_{off} equals to 50 µsec, SEC is remarkably increased. The reason behind that at higher pulse duration, discharge energy is created for a prolonged duration, liberated more heat energy, which transform into arcing and deposition of graphene nanoparticles as well as carbon over the machined cavity, as evidenced in EDX plot provided in Fig. 25. As an outcome, electrode erosion process is significantly disturbed and, thereof, large amount of energy is consumed with the increase in PTR under graphene mixed dielectric. It is summarized that minimum value of PTR (0.5) is appreciable for the graphene mixed dielectric during machining of Ti–6Al–4V via EDM process.

3.3.5. Effect of graphene concentration

Just like the other plots, the impact of graphene concentration on SEC is also discussed in Fig. 22, considering the processing of Ti–6Al–4V through the EDM setup. Initially, SEC decreases when the concentration of nanopowder is altered from 0.3 g/L to 0.5 g/L. When the concentration of powder rises in the dielectric liquid, the scattering of sparks increases, and breakdown strength improves. Thus, MRR upsurges or

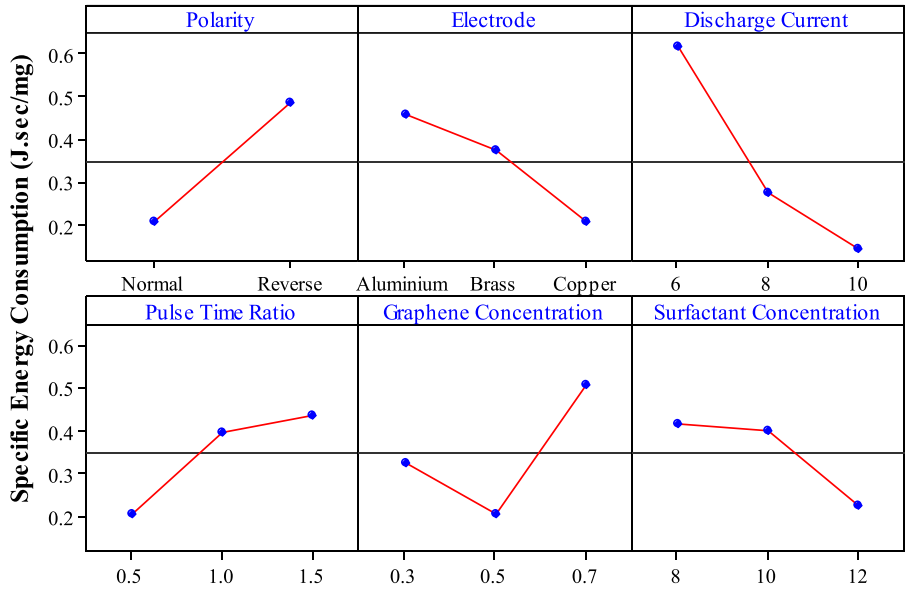

Fig. 22. Main effect plot for SEC against input parameters.

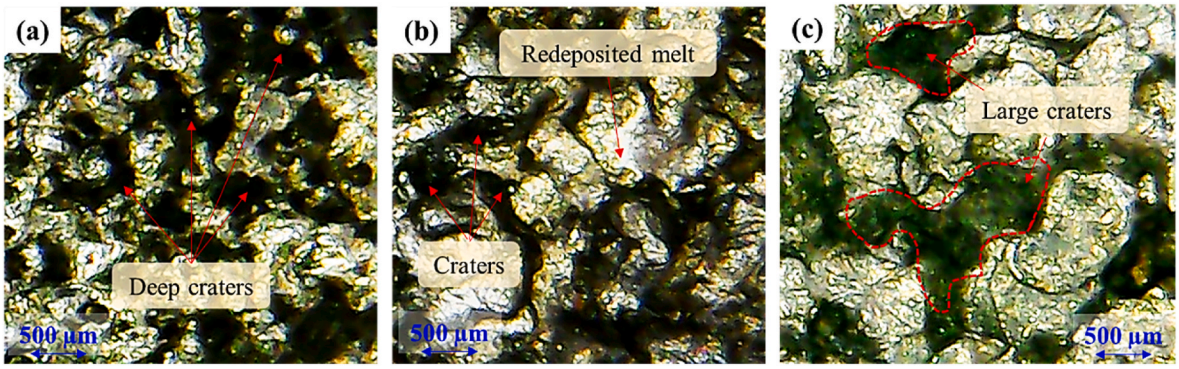

Fig. 23. Optical micrographs of specimen's surface against the three electrodes. (a) Al, (b) brass, (c) Cu.

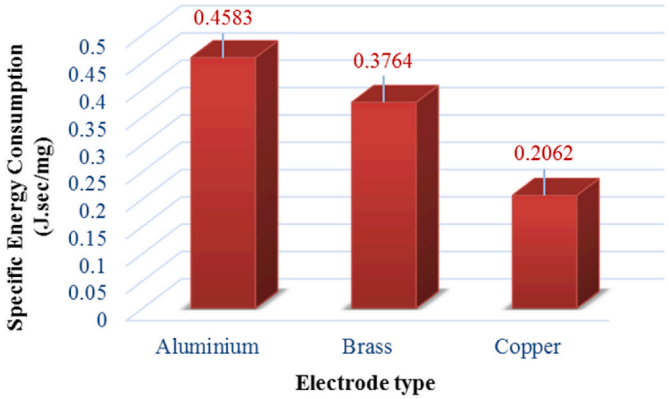

Fig. 24. Bar graph between electrode types versus SEC.

SEC declines. However, with the further addition of graphene powder in the RBO, SEC sharply increased. This is due to the development of the pool of particles in front of discharges which lowers the MRR. Therefore, SEC is uplifted. A comparative assessment of SEC is also developed using smallest and mean values against the parametric levels of graphene concentration, as seen in Fig. 26. Amongst the three powder concentrations, 0.5 g/L is the optimal value for getting a lower magnitude of SEC when EDM of the selected workpiece is undertaken.

3.3.6. *Effect of surfactant concentration*

The influence of different concentrations (8, 10, 12 g/L) of surfactant on SEC is also provided in Fig. 22. It can be noted that increase in S_C lowers the value of SEC. At 12 g/L, SEC is lowered as compared to the rest of the conditions. At higher S_C, suspension and agglomeration of particles are reduced. Therefore, each ionized particle gets a chance to strike the surface with equal ease. Eventually, the rate of material erosion is enhanced. As a result, the minimum value of SEC is achieved at a higher surfactant concentration when graphene nanoparticles are utilized with the rice bran oil. To sum up the discussion, the lower SEC is achieved when normal polarity is set against the copper electrode while EDM of elected Ti-alloy. The other optimum settings are DC = 10 A, PTR = 0.5, G_C = 0.5 g/L, and S_C = 12 g/L.

Taking the influence of six parameters mutually, the optimum settings, taken from DOE, for gaining higher magnitude of MRR, lower value of SR and SEC are tabulated in Table 10. According to the settings presented in Table 10, the normal polarity of EDM, graphene concentration (0.3 g/L), and surfactant concentration (8 g/L) have been proven to be the optimal one for each response. It is interesting to note that the optimal settings for both MRR and SEC are alike. As far as previously said responses are concerned, brass electrode, DC (10 A), and PTR (1.5) have appeared to be optimal conditions. However, the best electrode for improving the SR is named aluminium. Correspondingly, discharge

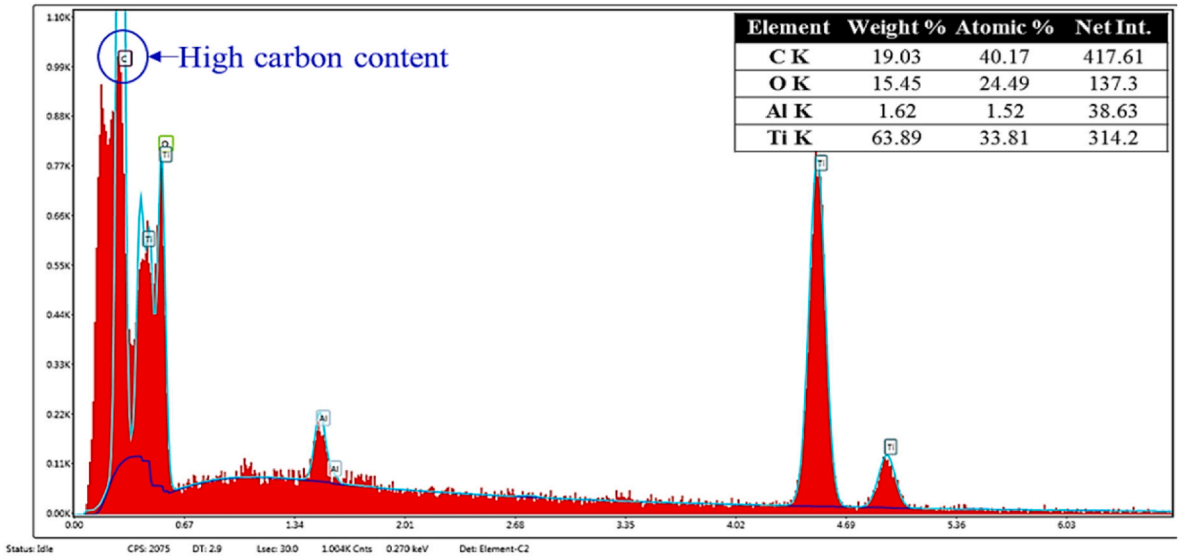

Fig. 25. EDX plot represents the elemental composition of a machined sample.

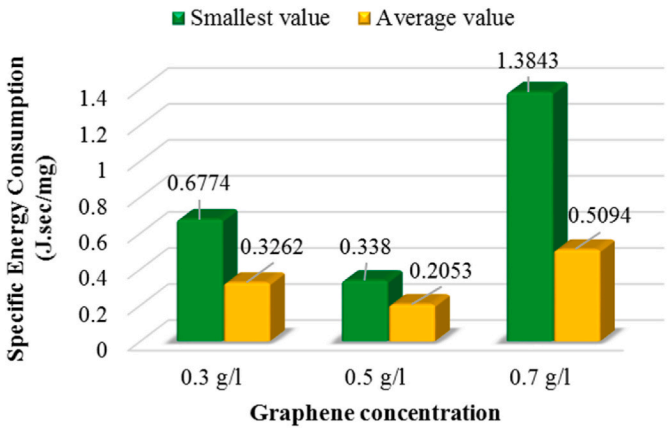

Fig. 26. Effect of graphene concentration on SEC for the EDM of Ti–6Al–4V.

current of 6 A is the favorable setting for attaining minimum SR. Moreover, 1st level (0.5) of PTR is an ideal condition for getting a good surface finish. The optimum combinations gathered in Table 10 have also been validated through confirmation runs. The results of these runs are compiled in Table 11. It has been observed that only 0.001 %, 0.069 %, and 0.129 % errors were noted in the value of MRR, SR, and SEC, respectively.

To further highlight the supremacy of the process, the current findings have been compared with the optimal results of traditional EDM setup, employing a mixture of kerosene dielectric and graphene nanoplatelets (see Fig. 27). The graphical analysis in Fig. 27 showed that proposed EDM setup (graphene-RBO) is outperformed in comparison to traditional EDM process. The MRR, SR, and SEC improved by 98.8 %, 0.68 %, and 93.99 % respectively when graphene-RBO mixed dielectric is engaged instead of conventional kerosene based EDM setup even after mixing graphene in kerosene. Hence, use of graphene-RBO combination during EDM of Ti-alloy is far better than that of conventional EDM setup to fulfill the need of sustainable manufacturing.

4. The sustainability aspect of EDM process

Manufacturing is the sector that consumes the most renewable and non-renewable resources. It not only changes raw materials into useable products but also generates a significant amount of waste. The waste produced during the manufacturing process has a negative impact on the ecosystem (Sana et al., 2024a). For example, Carbon dioxide (CO_2) emissions are a significant contributor to global climate change and can have a range of negative impacts on the environment. When CO_2 is escaped out into the air, it behaves as a greenhouse gas, blocking heat energy and triggering the Earth's average temperature to rise, as shown in Fig. 28. This result in changing the weather behavior, increasing sea levels, melting of glaciers, and severe natural cataclysms (Ahmed et al., 2020). Additionally, above the threshold level concentration of CO_2 in the atmosphere can also lead to acid rain, which cannot only disturb the aquatic life-style but also alter the biodiversity on the earth (Lee et al., 2021). For that reason, sustainability is essential in up-surging efficiency, reducing waste, and shielding the atmosphere from any damage.

EDM process is an environmentally friendly manufacturing approach due to comprising various sustainability aspects. It is already known that EDM setup can easily be used for hard-to-cut materials, which makes it a suitable candidate for reducing the need of multiple machining

Table 11
Findings of confirmation experiment.

Responses	Experimental values	Observed values	Error (%)
MRR	58.58	58.58	0.001 %
SR	2.89	2.88	0.069 %
SEC	0.0077	0.008	0.129 %

Table 10
Optimum parametric combinations for MRR, SR, and SEC.

Response' name	Input parameters					
	Polarity	Electrode type	Discharge current	Pulse time ratio	Graphene concentration	Surfactant concentration
MRR	Normal	Brass	10	1.5	0.3	8
SR		Al	6	0.5	0.3	8
SEC		Brass	10	1.5	0.3	8

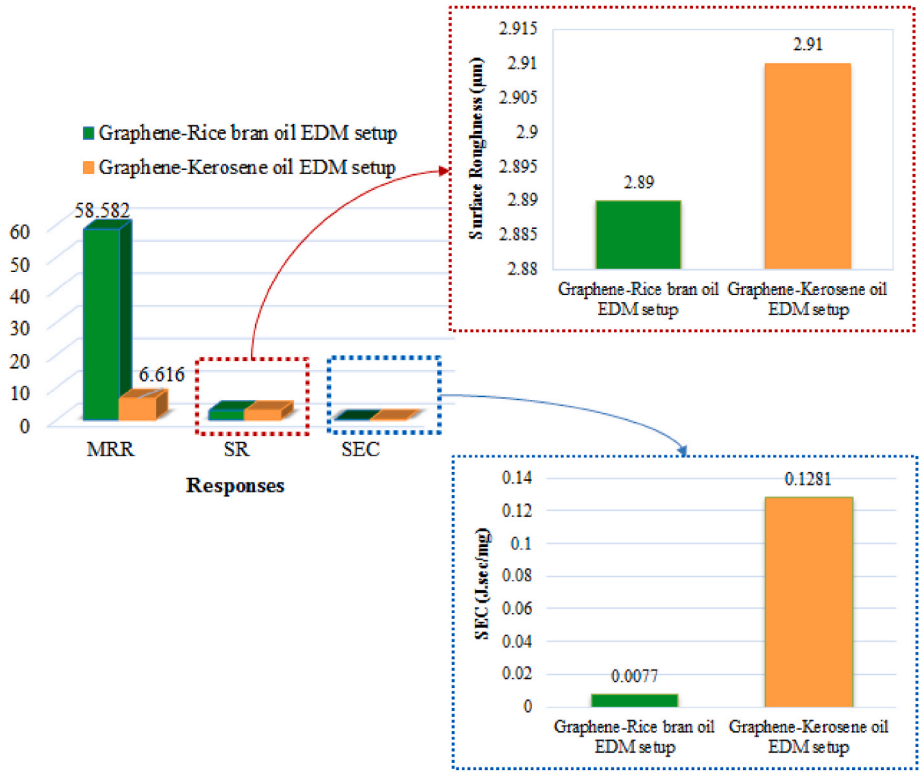

Fig. 27. Graphical analysis of graphene-RBO mixed EDM setup with the graphene-kerosene oil based EDM.

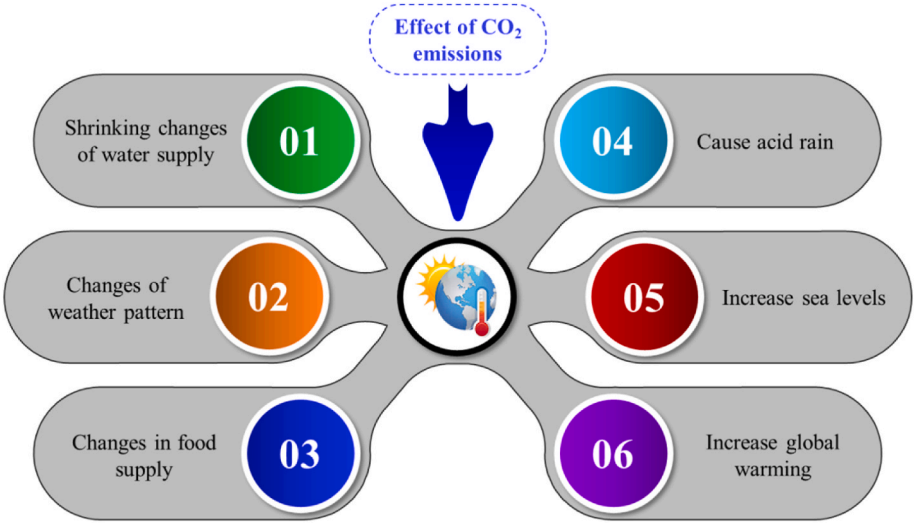

Fig. 28. Various implications of CO_2 emissions.

operations, ultimately turning into a cost-effective process. Moreover, it also consumes low non-renewable resources such as oil and gas, and thus is used for the production of sustainable products. Therefore, EDM is an encouraging machinery for sustainable manufacturing practices (Ming et al., 2021; Singh and Sharma, 2016). Although EDM has great benefits, it has several environmental impacts. For instance, EDM generates a large amount of surplus in the form of debris/sludge, which can be difficult to dispose of safely. In addition, EDM can consume large amounts of energy, which can promote greenhouse gas (CO_2) emissions and other environmental problems. The use of efficient machines and optimized machining factors can lead to attain low energy consumption and CO_2 emissions (Reddy et al., 2021). A similar findings have been reported by Niamat et al. (2019). In this work, three responses have been assayed against six input variables such as discussed earlier. Contributions towards sustainable machining are made by each response.

This could involve achieving specific values for MRR, SEC, and SR, which can lead to high throughput rate, low energy consumption, and good quality products. For making a function of performance metrics with sustainability, Eq. 9 is derived.

$$Sustainability = \begin{cases} \text{Maximize } MRR \\ \text{Minimize } SR \\ \text{Minimize } SEC \\ \text{Minimize } CO_2 \end{cases} \quad (4b)$$

5. Reduction in carbon dioxide emissions

The effect of CO_2 release on the environment has been studied in the former section. This part covers the computation of relative carbon dioxide emissions (R_{CE}) with respect to kerosene. The guidelines of intergovernmental panel on climate change (IPCC) was followed for this purpose (Krey et al., 2014). The CO_2 emissions for both biodegradable (rice bran oil) and conventional (kerosene) dielectrics were primarily determined by multiplying the SEC values with the CO_2 emission factor (0.1894 μgCO_2/J), taken from the IPCC's report. Rice bran oil yielded 1.4548 μgCO2/J emissions. The CO_2 emissions were also determined for the conventional dielectric, resulting in a maximum value of 4035.15 μgCO2/J. The findings of CO_2 emissions versus the two dielectrics (RBO and kerosene oil) are shown in Fig. 29. The outcomes were obtained considering brass-electrode because it provided lowest SEC value during EDM of Ti-alloy (see Table 10). For computing R_{CE}, the aforesaid CO_2 emission value for kerosene oil was taken as reference. The R_{CE} value was computed from the mathematical expression given in Eq. 10.

For the EDM cutting of Ti–6Al–4V, it was found that rice bran oil provided R_{CE} value equal to 99.96% compared to kerosene dielectric. Hence, it can be said that kerosene oil emits a greater amount of CO_2 and should be classified as a non-biodegradable oil.

$$R_{CE} = \left(\frac{CO_2 \text{ emission for kerosene dielectric} \; - \; CO_2 \text{ emission for rice bran oil}}{CO_2 \text{ emission for kerosene dielectric}} \right) \times 100 \tag{5b}$$

6. Modelling the EDM process by ANN and multi-objective optimization by NSGA-II

In this study, a three-layered shallow artificial neural network (ANN) model is developed to accurately model MRR, SR and SEC of the EDM process. To split the data into training, and testing datasets, a split ratio of 0.8, and 0.2 is utilized respectively. The hidden layer neurons are varied from 6 to 15, that is 1–2.5 times of input variables and a reasonably wide range to determine the optimal number of hidden layer neurons (Sana et al., 2024b). The hidden layer uses the tangent sigmoidal activation function, while the output layer uses the linear activation function. The Levenberg-Marquardt algorithm is utilized to optimize the parameter values, including weights and biases. Fig. 30**(a, b)** shows the predictive performance of the ANN models having different hidden layer neurons for training and testing dataset and are constructed for MRR, SR and SEC of EDM process. The predictive performance of the ANN models is gauged by R^2 and RMSE. Referring to Fig. 30**(a, b)** that shows the impact of varying hidden layer neurons on R^2 and RMSE value for three output variables of EDM process. Closely comparing the R^2 and RMSE for training and testing datasets as function of hidden layer neurons, it is found that ANN model having six hidden layer neurons has comparatively better R^2 and RMSE for MRR and SEC. Whereas, ANN model with eight hidden layer neurons shows the superior modelling performance for SR. Thus, the performance measures for the ANN model for MRR are as follows: R^2_train = 1, RMSE_train = 0.00034 mg/min, R^2_test = 0.94, RMSE_test = 3.25 mg/min. For SR, the performance measures are: R^2_train = 1, RMSE_train = 1.1 x 10^{-15} μm, R^2_test = 0.99, RMSE_test = 0.27 μm. Whereas the performance measures for SEC are as follows: R^2_train = 0.96, RMSE_train = 0.069 J s/mg, R^2_test = 0.97, RMSE_test = 0.064 J s/mg.

The multi-objective optimization problem that attempts to maximize MRR and minimize SR and SEC is formulated by integrating the trained ANN models in it and the optimal solution is explored from the operating ranges of the input variables as mentioned in Table 8. The multi-objective optimization problem is solved by NSGA-II method and multiple solutions are obtained satisfying the objective and the applied constraints. The optimal solution is selected by TOPSIS technique as presented on Fig. 30**(c)**. The optimized operating values for the input variables are as follows: Polarity = normal, ET = Brass, DC = 10 A, PTR = 1.47, G_C = 0.54 (g/liter) and S_C = 8.74 (g/liter). Whereas the optimal values for the output variables of the EDM process are: MRR = 10.56 mg/min, SR = 5.72 μm and SEC = 0.010 J s/mg. The aforementioned values have been further validated by the aid of confirmation trials.

The optimal setting put forwarded by the TOPSIS method has been further validated by performing confirmation runs. The results of these runs are presented in Table 12. It has been perceived that the findings from these runs closely matched the optimal results. For instance, after validation, the values of MRR, SR, and SEC were measured as 10.58 mg/min, 5.70 μm, and 0.0099 J s/mg SEC, respectively. In order to determine the percentage improvement in the magnitude of these responses, the aforementioned results were compared with the average value of each response data. The results indicated that there was a predicted improvement of 133.66% in the value of MRR, 11.05% in SR, and 35-times in SEC. However, Table 13 represents the comparison of current study findings with the published literature.

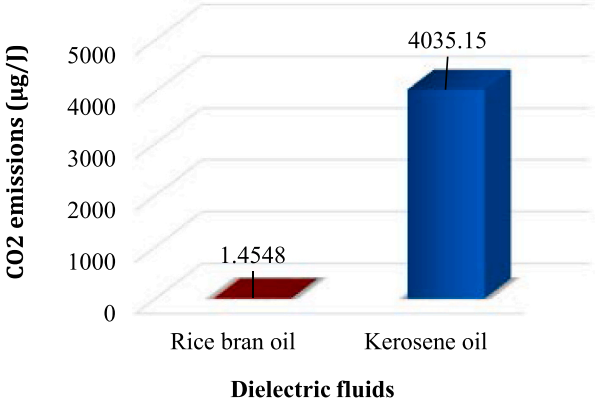

Fig. 29. Variations of CO_2 emissions recorded for the distinct dielectric oils.

7. Conclusions

The current study has comprehensively explored the potential of nano graphene-based rice bran oil as potential alternate to the traditional dielectric to make EDM process cleaner and sustainable. Three important aspects i.e. MRR, SEC and SR were investigated which in turn determine the productivity, energy consumption and surface quality of the machined component. Experimentation was performed using Taguchi's experimental approach. Experimental findings have been thoroughly discussed based on the underlying phenomena. ANN approach has been employed for efficient modelling of the process responses. Finally parametric optimization has also been carried out using NSGA-II and TOPSIS techniques. On account of the current research, the following inferences are drawn.

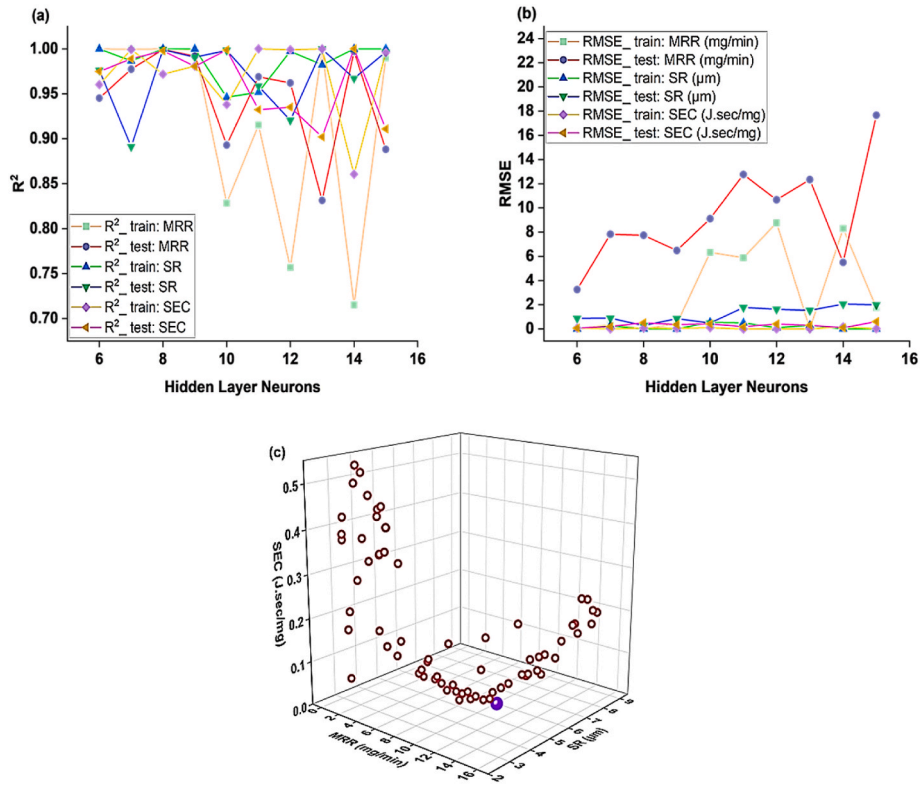

Fig. 30. ANN and NSGA-II based modelling and optimization analysis for EDM process. The predictive performance of ANN models with respect to hidden layer neurons for training and testing datasets are shown in (a) and (b) respectively. (c) Multi-objective optimization analysis by genetic algorithm is conducted and the optimal solution selected by TOPSIS technique is presented by solid sphere in (c).

Table 12
Outcomes of confirmation experiment.

Sr. No.	Settings	MRR (mg/min)	SR (μm)	SEC (J. sec/mg)
1.	(Optimal) Polarity = normal, Electrode type = Brass, Discharge current = 10 A, Pulse time ratio = 1.47, Graphene conc. = 0.54 g/L Surfactant conc. = 8.74 g/L	10.58	5.70	0.0099
2.	Average magnitudes of responses found during whole experimentation	4.5279	6.33	0.3470
Percentage improvement in response magnitude		133.66 %	11.05 %	35 times

Table 13
Comparison of current study with literature.

References	Alloys	MRR	SR	SEC
Current study	Ti–6Al–4V	58.58	2.89	0.01
Umanath and Devika (2018)	Ti–6Al–4V	7.36	2.27	–
Kolli and Kumar (2015b)	Ti–6Al–4V	6.84	1.95	–
Nair et al. (2019)	Ti–6Al–4V	3.207	2.38	–
Kao et al. (2010)	Ti–6Al–4V	23.49	4.74	–

1. Nano graphene-based rice bran oil has proved to be a valuable substitute of kerosene in EDM of Ti–6Al–4V for making the process sustainable. In comparison to the traditional dielectric the unique combination of rice bran oil and nano graphene has provided significantly better results in terms of MRR and SEC without compromising the surface quality.
2. The performance of rice bran oil is found to be better in contest to kerosene owing to its high thermal conductivity, viscosity and dielectric constant in all perspectives (MRR, SR, and SEC). The MRR, SR, and SEC improved by 98.8 %, 0.68 %, and 93.99 % respectively when graphene-RBO mixed dielectric is engaged instead of conventional kerosene based EDM setup even after mixing graphene in kerosene.
3. The nano-platelets of graphene bear an appreciable role during the cutting of Ti-alloy. During the discharging process nano-graphene generates a large number of ions that not only enrich the plasma channel but also facilitates the electric sparks dissemination. As a result, workpiece-electrode gap increases, and bridging phenomenon occurs in the direction of the current flow which makes the discharging process steady/stable. This leads to an increase in the cutting rate, improvement in the surface finish, and reduction in energy consumption. It has been observed that addition of the nano graphene which has high thermal and electrical conductivities further amplify the cutting proficiency of the rice bran oil.
4. The performance of brass electrode has been observed best amongst the three electrodes in terms of MRR and SEC for EDM of Ti-alloy under RBO dielectric. The thermal conductivity of the brass electrode is lowest in comparison to Cu and Al which ensures the availability of heat in the workpiece-electrode gap rather to be sunk by the electrode body. Thus, heat flux is being absorbed or faced by the target material which in turn translates in higher MRR and lesser SEC. Whereas, for the case of surface roughness, Al electrode has performed better. The low melting temperature and density of aluminium than the other tools are the reason for providing good surface finish. Because both the said characteristics of Al causes rapid wear of the electrode during the discharging process. Subsequently the workpiece-electrode gap is increased which reduces the intensity of the

sparking in the cutting regime. Thus, smaller amounts of material are removed from the workpiece producing shallow craters resulting in better surface finish.

5. The concentration of surfactant plays differently for MRR and other responses in nano graphene based EDM. The first level (8 g/L) of this parameter provides the higher value of MRR whereas the third level (12 g/L) resulted in better surface quality and SEC. The addition of surfactant has dielectric conductivity and triggered the discharge energy to penetrate more effectively into the cutting cavity which improves the cutting proficiency. The high value of its concentration (12 g/L) disseminates the powder particles more effectively and a uniform dispersion of discharge sites is realized in the cutting regime which creates smoother surface with lesser energy consumption.
6. The normal tool polarity has demonstrated appreciable results in terms of MRR, SR, and SEC in comparison to the reverse one in graphene-rice bran mixed EDM of Ti-alloy.
7. The trends of DC and PTR are similar for the set responses. They have showed nearly a liner relation for defined output parameters. High value of both variables has produced grater amount of MRR with lesser SEC. However, for SR, smaller values of these variables show improved surface finish.
8. As long as the graphene concentration is considered, 0.3 g/L, 0.5 g/L, and 0.7 g/L have been realized as favorable for MRR, SEC, and SR, respectively. At 0.3 g/L, the rate of powder's suspension and agglomeration is lesser. Thus, high MRR has been obtained at the said graphene concentration. When the concentration of graphene increases to a maximum value, surface roughness is reduced because spark energy changes into several patches by increasing the electrode-workpiece gap, making bridges from tool to machined cavity and scattering heat energy more uniformly. Therefore, SR has improved at 0.7 g/L. At the middle condition (0.5 g/L) of graphene concentration, SEC value has been greatly dropped due to lowering of breakdown strength and significant expansion of plasma density over the workpiece surface.
9. The study also revealed that the use of novel graphene-based rice bran oil produced 99.96% lesser CO_2 emissions as compared to the traditional dielectric, indicating that the proposed combination is an excellent choice for making EDM process sustainable.
10. The successful development of ANN based models is another appreciable aspect of this work which allows the standardization of EDM processing performance. All the proposed models have R^2 value greater than 0.9 which is proof of their adequacy in terms of accurate prediction. Moreover, the magnitudes of RSME are also very small for all the models. These findings indicate that the ANN model was effectively trained, tested, and justified.
11 The EDM performance of Ti–6Al–4V under nano graphene-based rice bran oil has also been optimized using NSGA-II driven multi-objective optimization technique. Multiple solutions have been estimated however, TOPSIS approach is employed for selecting the optimal operating setting (as mentioned in Table 12). This proposed setting has been further confirmed by performing confirmation runs. As an outcome, 113.66%, 11.05%-, and 35-times improvements were noticed in the responses' value, respectively, when comparison has been made with the average value of each response obtained during the whole experimentation.

The findings of the present study are worth considering for industries like aerospace, defense and biomedical wherein EDM is commonly used for machining of difficult-to-cut materials. The adoption of the proposed combination of input variables under novel blend of nanographene and rice bran oil not only ensures the productivity improvement but also contributes for making the process sustainable as well. A notable decrease in the CO_2 emissions using the proposed methodology will surely help industry to realize the goal of Net-Zero. Moreover, the issue of toxic fumes generation due to the thermal breakdown of the traditional dielectric molecules during discharging phenomenon has also been resolved, which is a serious concern for both environment and operator's health. Another valuable contribution of the study is the successful ANN based modelling of the process which significantly reduces the need for extensive experimentation. Considering that EDM is costly and stochastic process, therefore, the development of ANN based models enables industries to select appropriate levels of control variable without performing laborious experimentation. These salient features of the study clearly demonstrate its emphasis on making the process practical and sustainable for the industry.

Future work

The cutting potential of nano-graphene mixed rice bran oil has been comprehensively investigated for making the EDM of Ti6Al4V sustainable. However, the work can be extended considering the other types of biodegradable dielectrics employing the same additive to seek further improvement in the process. The application of electrode's treatment is another potential are which can be targeted in future using the same dielectric and additive. Analytical modelling of the process while engaging the proposed dielectric mixture of nano graphene and rice bran oil could be another valuable future direction.

CRediT authorship contribution statement

Kashif Ishfaq: Writing – original draft, Resources, Investigation, Data curation, Conceptualization. **Muhammad Asad:** Writing – original draft, Visualization, Software, Methodology, Formal analysis, Data curation. **Waqar Muhammad Ashraf:** Writing – review & editing, Validation, Software, Methodology, Formal analysis. **Muhammad Sana:** Writing – review & editing, Writing – original draft, Software, Methodology, Investigation, Formal analysis. **Saqib Anwar:** Writing – review & editing, Visualization, Resources, Funding acquisition, Data curation. **Wei Zhang:** Writing – review & editing, Software, Formal analysis. **Vivek Dua:** Writing – review & editing, Visualization, Supervision, Project administration.

Declaration of competing interest

The authors declare that they have no known competing financial interests or personal relationships that could have appeared to influence the work reported in this paper.

Data availability

Data will be made available on request.

Acknowledgement

The authors appreciate the support from Researchers Supporting Project Number (RSPD2024R702), King Saud University, Riyadh, Saudi Arabia.

References

Abu Qudeiri, J.E., Mourad, A.-H.I., Ziout, A., et al., 2018. Electric discharge machining of titanium and its alloys: review. Int. J. Adv. Des. Manuf. Technol. 96, 1319–1339. https://doi.org/10.1007/s00170-018-1574-0.

Ahmed, N., Anwar, S., Ishfaq, K., et al., 2019. The potentiality of sinking EDM for micro-impressions on Ti-6Al-4V: keeping the geometrical errors (axial and radial) and other machining measures (tool erosion and work roughness) at minimum. Sci. Rep. 9, 17218 https://doi.org/10.1038/s41598-019-52855-6.

Ahmed, Ali K., Ahmad, M.I., Yusup, Y., 2020. Issues, impacts, and mitigations of carbon dioxide emissions in the building sector. Sustainability 12, 7427. https://doi.org/10.3390/su12187427.

Arif, U., Ali Khan, I., Hasan, F., 2022. Green and sustainable electric discharge machining: a review. In: Advances in Materials and Processing Technologies, pp. 1–75. https://doi.org/10.1080/2374068X.2022.2108599.

Ashraf, W.M., Rafique, Y., Uddin, G.M., et al., 2022. Artificial intelligence based operational strategy development and implementation for vibration reduction of a supercritical steam turbine shaft bearing. Alex. Eng. J. 61, 1864–1880. https://doi.org/10.1016/j.aej.2021.07.039.

Azhiri, R.B., Jadidi, A., Teimouri, R., 2020. Electrical discharge turning by assistance of external magnetic field, part II: study of surface integrity. International Journal of Lightweight Materials and Manufacture 3, 305–315. https://doi.org/10.1016/j.ijlmm.2020.03.002.

Bajaj, R., Dixit, A.R., Tiwari, A.K., 2020. Machining performance enhancement of powder mixed electric discharge machining using Green dielectric fluid. J. Braz. Soc. Mech. Sci. Eng. 42, 512. https://doi.org/10.1007/s40430-020-02597-8.

Basha, S.M., Dave, H.K., Patel, H.V., 2021. Experimental investigation of jatropha curcas bio-oil and biodiesel in electric discharge machining of Ti-6Al-4V. Mater. Today: Proc. 38, 2102–2109. https://doi.org/10.1016/j.matpr.2020.04.536.

Chakraborty, T., Sahu, D.R., Mandal, A., Acherjee, B., 2023. Feasibility of Jatropha and Rice bran vegetable oils as sustainable EDM dielectrics. Mater. Manuf. Process. 38, 50–63. https://doi.org/10.1080/10426914.2022.2089891.

Chukka, N.D.K.R., Arivumangai, A., Kumar, S., et al., 2022. Environmental impact and carbon footprint assessment of sustainable buildings: an experimental investigation. Adsorpt. Sci. Technol. 2022, 1–8. https://doi.org/10.1155/2022/8130180.

Das, S., Paul, S., Doloi, B., 2020. Feasibility investigation of neem oil as a dielectric for electrical discharge machining. Int. J. Adv. Des. Manuf. Technol. 106, 1179–1189. https://doi.org/10.1007/s00170-019-04736-5.

Das, S., Paul, S., Doloi, B., 2021. Assessment of the impacts of bio-dielectrics on the textural features and recast-layers of EDM-surfaces. Mater. Manuf. Process. 36, 245–255. https://doi.org/10.1080/10426914.2020.1832678.

Deb, K., 1999. An introduction to genetic algorithms. Sadhana 24, 293–315. https://doi.org/10.1007/BF02823145.

Deb, K., Pratap, A., Agarwal, S., Meyarivan, T., 2002. A fast and elitist multiobjective genetic algorithm: nsga-II. IEEE Trans. Evol. Comput. 6, 182–197. https://doi.org/10.1109/4235.996017.

Farooq, M.U., Bhatti, H.A., Asad, M., et al., 2022. Surface generation on titanium alloy through powder-mixed electric discharge machining with the focus on bioimplant applications. Int. J. Adv. Des. Manuf. Technol. 122, 1395–1411. https://doi.org/10.1007/s00170-022-09927-1.

Feng, J.Q., Hays, D.A., 2003. Relative importance of electrostatic forces on powder particles. Powder Technol. 135–136, 65–75. https://doi.org/10.1016/j.powtec.2003.08.005.

Fraterrigo, Garofalo S., Tommasi, T., Fino, D., 2021. A short review of green extraction technologies for rice bran oil. Biomass Conversion and Biorefinery 11, 569–587. https://doi.org/10.1007/s13399-020-00846-3.

Garg, A., Lam, J.S.L., 2016. Modeling multiple-response environmental and manufacturing characteristics of EDM process. J. Clean. Prod. 137, 1588–1601. https://doi.org/10.1016/j.jclepro.2016.04.070.

Ge, Z., Yang, L., Xiao, F., et al., 2018. Graphene family nanomaterials: properties and potential applications in dentistry. International Journal of Biomaterials 1–12. https://doi.org/10.1155/2018/1539678, 2018.

Goyal, A., Pandey, A., Sharma, P., 2018. Investigation of surface roughness for Inconel 625 using wire electric discharge machining. IOP Conf. Ser. Mater. Sci. Eng. 377, 012109 https://doi.org/10.1088/1757-899X/377/1/012109.

Hasçalık, A., Çaydaş, U., 2007. Electrical discharge machining of titanium alloy (Ti–6Al–4V). Appl. Surf. Sci. 253, 9007–9016. https://doi.org/10.1016/j.apsusc.2007.05.031.

Heydari-Bafrooei, E., Ensafi, A.A., 2019. Typically used carbon-based nanomaterials in the fabrication of biosensors. In: Electrochemical Biosensors. Elsevier, pp. 77–98.

Ishfaq, K., Asad, M., Anwar, S., et al., 2020. A comprehensive analysis of the effect of graphene-based dielectric for sustainable electric discharge machining of Ti-6Al-4V. Materials 14, 23. https://doi.org/10.3390/ma14010023.

Ishfaq, K., Sana, M., Waseem, M.U., et al., 2023a. Enhancing EDM machining precision through deep cryogenically treated electrodes and ANN modelling approach. Micromachines 14, 1536. https://doi.org/10.3390/mi14081536.

Ishfaq, K., Ahmad, N., Maqsood, M.A., et al., 2023b. A systematic study to achieve cleaner and sustainable manufacturing process by using bio-degradable dielectrics. Sustainable Materials and Technologies 37, e00685. https://doi.org/10.1016/j.susmat.2023.e00685.

Ishfaq, K., Sana, M., Kumar, M.S., et al., 2023c. Optimizing the contributing electro-erosive discharge parameters for reducing the electrode wear and geometric dimensional deviation in EDM of Ti-based superalloy. Proc. Inst. Mech. Eng., Part B: Journal of Engineering Manufacture 09544054231205333. https://doi.org/10.1177/09544054231205333.

Ishfaq, K., Sana, M., Ashraf, W.M., 2023d. Artificial intelligence–built analysis framework for the manufacturing sector: performance optimization of wire electric discharge machining system. Int. J. Adv. Manuf. Technol. 128, 5025–5039. https://doi.org/10.1007/s00170-023-12191-6.

Ishfaq, K., Sana, M., Waseem, M.U., et al., 2024. Circular usage of waste cooking oil towards green electrical discharge machining process with lower carbon emissions. Int. J. Adv. Manuf. Technol. https://doi.org/10.1007/s00170-024-13322-3.

Joshi, A.Y., Joshi, A.Y., 2019a. A systematic review on powder mixed electrical discharge machining. Heliyon 5, e02963. https://doi.org/10.1016/j.heliyon.2019.e02963.

Joshi, A.Y., Joshi, A.Y., 2019b. A systematic review on powder mixed electrical discharge machining. Heliyon 5, e02963. https://doi.org/10.1016/j.heliyon.2019.e02963.

Kah, P., Vimalraj, C., Martikainen, J., Suoranta, R., 2015. Factors influencing Al-Cu weld properties by intermetallic compound formation. Int. J. Mech. Mater. Eng. 10, 10. https://doi.org/10.1186/s40712-015-0037-8.

Kao, J.Y., Tsao, C.C., Wang, S.S., Hsu, C.Y., 2010. Optimization of the EDM parameters on machining Ti–6Al–4V with multiple quality characteristics. Int. J. Adv. Manuf. Technol. 47, 395–402. https://doi.org/10.1007/s00170-009-2208-3.

Khan, A.A., 2008. Electrode wear and material removal rate during EDM of aluminum and mild steel using copper and brass electrodes. Int. J. Adv. Des. Manuf. Technol. 39, 482–487. https://doi.org/10.1007/s00170-007-1241-3.

Khan, D.A., Hameedullah, M., 2011. Effect of tool polarity on the machining characteristics in electric discharge machining of silver steel and statistical modelling of the process. Int. J. Eng. Sci. 3, 5001–5010.

Khan, A.A., Azmi, N.W., Odenan, M.A., Zain, Z.M., 2015. Effect of powder concentration on EDM performance during machining mild steel. Adv. Mater. Res. 1115, 7–11. https://doi.org/10.4028/www.scientific.net/AMR.1115.7.

Kolli, M., Adepu, K., 2016. Optimization of the parameters for the surfactant-added EDM of a Ti–6Al–4V alloy using the GRA-Taguchi method. Materiali in tehnologije 50, 229–238. https://doi.org/10.17222/mit.2014.249.

Kolli, M., Kumar, A., 2015a. Effect of dielectric fluid with surfactant and graphite powder on Electrical Discharge Machining of titanium alloy using Taguchi method. Engineering Science and Technology, an International Journal 18, 524–535. https://doi.org/10.1016/j.jestch.2015.03.009.

Kolli, M., Kumar, A., 2015b. Effect of dielectric fluid with surfactant and graphite powder on Electrical Discharge Machining of titanium alloy using Taguchi method. Engineering Science and Technology, an International Journal 18, 524–535. https://doi.org/10.1016/j.jestch.2015.03.009.

Krey, V., Masera, O., Blanforde, G., et al., 2014. Annex II: Metrics & Methodology. United Kingdom and New York, NY, USA.

Leão, F.N., Pashby, I.R., 2004. A review on the use of environmentally-friendly dielectric fluids in electrical discharge machining. J. Mater. Process. Technol. 149, 341–346. https://doi.org/10.1016/j.jmatprotec.2003.10.043.

Lee, J.Y., Marotzke, J., Bala, G., et al., 2021. IPCC. Climate Change 2021: the Physical Science Basis.

Leppert, T., 2018. A review on ecological and health impacts of electro discharge machining (EDM). In: AIP Conference Proceedings 2017. AIP Publishing LLC, 020014.

Li, M., Cai, L., Zhao, J., 2021. Research on discharge characteristics of working mediums of electric discharge machining. Proc. IME B J. Eng. Manufact. 235, 34–40. https://doi.org/10.1177/0954405420951093.

Madurani, K.A., Suprapto, S., Machrita, N.I., et al., 2020. Progress in graphene synthesis and its application: history, challenge and the future outlook for research and industry. ECS Journal of Solid State Science and Technology 9, 093013. https://doi.org/10.1149/2162-8777/abbb6f.

MangapathiRao, K., Vinaykumar, D., Chandra Shekar, K., Kumar, R.R., 2021. Investigation and analysis of EDM process – a new approach with Al2O3 nano powder mixed in sunflower oil. IOP Conf. Ser. Mater. Sci. Eng. 1057, 012059 https://doi.org/10.1088/1757-899X/1057/1/012059.

Ming, W., Shen, F., Zhang, G., et al., 2021. Green machining: a framework for optimization of cutting parameters to minimize energy consumption and exhaust emissions during electrical discharge machining of Al 6061 and SKD 11. J. Clean. Prod. 285, 124889 https://doi.org/10.1016/j.jclepro.2020.124889.

Mishra, B.P., Routara, B.C., 2020. Evaluation of technical feasibility and environmental impact of Calophyllum Inophyllum (Polanga) oil based bio-dielectric fluid for green EDM. Measurement 159, 107744. https://doi.org/10.1016/j.measurement.2020.107744.

Modica, F., Marrocco, V., Copani, G., Fassi, I., 2011. Sustainable micro-manufacturing of micro-components via micro electrical discharge machining. Sustainability 3, 2456–2469. https://doi.org/10.3390/su3122456.

Moudood, M.A., Sabur, A., Ali, M.Y., Jaafar, I.H., 2015. Effect of gap voltage and pulse-on time on material removal rate for electrical discharge machining of Al2O3. Adv. Mater. Res. 1115, 3–6. https://doi.org/10.4028/www.scientific.net/AMR.1115.3.

Muthuramalingam, T., Mohan, B., 2015. A review on influence of electrical process parameters in EDM process. Arch. Civ. Mech. Eng. 15, 87–94. https://doi.org/10.1016/j.acme.2014.02.009.

Muttamara, A., Kanchanomai, C., 2016. Effect of carbon in the dielectric fluid and workpieces on the characteristics of recast layers machined by electrical discharge machining. Metall. Mater. Trans. 47, 3248–3255. https://doi.org/10.1007/s11661-016-3452-4.

Nair, S., Dutta, A., Narayanan, R., Giridharan, A., 2019. Investigation on EDM machining of Ti6Al4V with negative polarity brass electrode. Mater. Manuf. Process. 34, 1824–1831. https://doi.org/10.1080/10426914.2019.1675891.

Ni, T., Liu, Q., Wang, Y., et al., 2021. Research on material removal mechanism of micro-EDM in deionized water. Coatings 11, 322. https://doi.org/10.3390/coatings11030322.

Niamat, M., Sarfraz, S., Ahmad, W., et al., 2019. Parametric modelling and multi-objective optimization of electro discharge machining process parameters for sustainable production. Energies 13, 38. https://doi.org/10.3390/en13010038.

Nieslony, P., Wojciechowski, S., Gupta, M.K., et al., 2023. Relationship between energy consumption and surface integrity aspects in electrical discharge machining of hot work die steel. Sustainable Materials and Technologies 36, e00623. https://doi.org/10.1016/j.susmat.2023.e00623.

Papazoglou, E.L., Karmiris-Obratański, P., Leszczyńska-Madej, B., Markopoulos, A.P., 2021. A study on electrical discharge machining of titanium Grade2 with experimental and theoretical analysis. Sci. Rep. 11, 8971. https://doi.org/10.1038/s41598-021-88534-8.

Paswan, K., Chattopadhyaya, S., Pramanik, A., 2021. Performance of graphene nanopowder with deionised water in EDM process. Mater. Sci. Forum 1026, 147–154. https://doi.org/10.4028/www.scientific.net/MSF.1026.147.

Peças, P., Henriques, E., 2008. Effect of the powder concentration and dielectric flow in the surface morphology in electrical discharge machining with powder-mixed dielectric (PMD-EDM). Int. J. Adv. Des. Manuf. Technol. 37, 1120–1132. https://doi.org/10.1007/s00170-007-1061-5.

Perumal, A., Kailasanathan, C., Stalin, B., et al., 2021. Evaluation of EDM process parameters on titanium alloy through Taguchi approach. Mater. Today: Proc. 45, 2394–2400. https://doi.org/10.1016/j.matpr.2020.10.737.

Philip, J.T., Mathew, J., Kuriachen, B., 2021. Transition from EDM to PMEDM – impact of suspended particulates in the dielectric on Ti6Al4V and other distinct material surfaces: a review. J. Manuf. Process. 64, 1105–1142. https://doi.org/10.1016/j.jmapro.2021.01.056.

Pradhan, M.K., 2013. Estimating the effect of process parameters on MRR, TWR and radial overcut of EDMed AISI D2 tool steel by RSM and GRA coupled with PCA. Int. J. Adv. Des. Manuf. Technol. 68, 591–605. https://doi.org/10.1007/s00170-013-4780-9.

Praveen, L., Geeta Krishna, P., Venugopal, L., Prasad, N.E.C., 2018. Effects of pulse ON and OFF time and electrode types on the material removal rate and tool wear rate of the Ti-6Al-4V Alloy using EDM machining with reverse polarity. IOP Conf. Ser. Mater. Sci. Eng. 330, 012083 https://doi.org/10.1088/1757-899X/330/1/012083.

Prihandana, G.S., Mahardika, M., Sriani, T., 2020. Micromachining in powder-mixed micro electrical discharge machining. Appl. Sci. 10, 3795. https://doi.org/10.3390/app10113795.

Priyadarsini, S., Mohanty, S., Mukherjee, S., et al., 2018. Graphene and graphene oxide as nanomaterials for medicine and biology application. Journal of Nanostructure in Chemistry 8, 123–137. https://doi.org/10.1007/s40097-018-0265-6.

Punia, S., Kumar, M., Siroha, A.K., Purewal, S.S., 2021. Rice bran oil: emerging trends in extraction, health benefit, and its industrial application. Rice Sci. 28, 217–232. https://doi.org/10.1016/j.rsci.2021.04.002.

Rajurkar, K.P., Hadidi, H., Pariti, J., Reddy, G.C., 2017. Review of sustainability issues in non-traditional machining processes. Procedia Manuf. 7, 714–720. https://doi.org/10.1016/j.promfg.2016.12.106.

Reddy, M.C., Venkata Rao, K., Suresh, G., 2021. An experimental investigation and optimization of energy consumption and surface defects in wire cut electric discharge machining. J. Alloys Compd. 861, 158582 https://doi.org/10.1016/j.jallcom.2020.158582.

S, R., Rjh, N., Sk, J., Krolczyk, G.M., 2021. A comprehensive review on research developments of vegetable-oil based cutting fluids for sustainable machining challenges. J. Manuf. Process. 67, 286–313. https://doi.org/10.1016/j.jmapro.2021.05.002.

Sana, M., Farooq, M.U., Anwar, S., Haber, R., 2023a. Predictive modelling framework on the basis of artificial neural network: a case of nano-powder mixed electric discharge machining. Heliyon 9, e22508. https://doi.org/10.1016/j.heliyon.2023.e22508.

Sana, M., Ishfaq, K., Waseem, M.U., et al., 2023b. A comparative study on the effect of deep and shallow cryogenic electrodes on tool wear rate and overcut with waste bio-oil in electric discharge machining. Int. J. Adv. Manuf. Technol. https://doi.org/10.1007/s00170-023-12860-6.

Sana, M., Asad, M., Farooq, M.U., et al., 2024a. Sustainable electric discharge machining using alumina-mixed deionized water as dielectric: process modelling by artificial neural networks underpinning net-zero from industry. J. Clean. Prod. 140926 https://doi.org/10.1016/j.jclepro.2024.140926.

Sana, M., Asad, M., Farooq, M.U., et al., 2024b. Machine learning for multi-dimensional performance optimization and predictive modelling of nanopowder-mixed electric discharge machining (EDM). Int. J. Adv. Manuf. Technol. https://doi.org/10.1007/s00170-024-13023-x.

Shams, S.R., Jahani, A., Kalantary, S., et al., 2021. The evaluation on artificial neural networks (ANN) and multiple linear regressions (MLR) models for predicting SO2 concentration. Urban Clim. 37, 100837 https://doi.org/10.1016/j.uclim.2021.100837.

Shen, Y., Liu, Y., Dong, H., et al., 2017. Parameters optimization for sustainable machining of Ti6Al4V using a novel high-speed dry electrical discharge milling. Int. J. Adv. Des. Manuf. Technol. 90, 2733–2740. https://doi.org/10.1007/s00170-016-9600-6.

Singaravel, B., Shekar, K.C., Reddy, G.G., Prasad, S.D., 2020. Experimental investigation of vegetable oil as dielectric fluid in Electric discharge machining of Ti-6Al-4V. Ain Shams Eng. J. 11, 143–147. https://doi.org/10.1016/j.asej.2019.07.010.

Singh, J., Sharma, R.K., 2016. Green EDM strategies to minimize environmental impact and improve process efficiency. J. Manuf. Sci. Prod. 16 https://doi.org/10.1515/jmsp-2016-0034.

Singh, AKr, Mahajan, R., Tiwari, A., et al., 2018. Effect of dielectric on electrical discharge machining: a review. IOP Conf. Ser. Mater. Sci. Eng. 377, 012184 https://doi.org/10.1088/1757-899X/377/1/012184.

Singh, N.K., Yadav, L., Lal, S., 2020. Experimental investigation for sustainable electric discharge machining with Pongamia and Jatropha as dielectric medium. Advances in Materials and Processing Technologies 1–20. https://doi.org/10.1080/2374068X.2020.1860499.

Tariq, R., Abatal, M., Bassam, A., 2022. Computational intelligence for empirical modeling and optimization of methylene blue adsorption phenomena using available local zeolites and clay of Morocco. J. Clean. Prod. 370, 133517 https://doi.org/10.1016/j.jclepro.2022.133517.

Tharian, B.K., Kumar, M., Dhanish, P.B., Manu, R., 2022. Effect of peak current on material removal rate during EDM of Ti–6Al–4V using cold treated brass electrode. In: Advances in Forming, Machining and Automation. Springer Nature, Singapore, pp. 243–251.

Tiwary, A.P., Pradhan, B.B., Bhattacharyya, B., 2015. Study on the influence of micro-EDM process parameters during machining of Ti–6Al–4V superalloy. Int. J. Adv. Des. Manuf. Technol. 76, 151–160. https://doi.org/10.1007/s00170-013-5557-x.

Uddin, G.M., Arafat, S.M., Ashraf, W.M., et al., 2020. Artificial intelligence-based emission reduction strategy for limestone forced oxidation flue gas desulfurization system. J. Energy Resour. Technol. 142 https://doi.org/10.1115/1.4046468.

Umanath, K., Devika, D., 2018. Optimization of electric discharge machining parameters on titanium alloy (ti-6al-4v) using Taguchi parametric design and genetic algorithm. MATEC Web Conf 172, 04007. https://doi.org/10.1051/matecconf/201817204007.

Valaki, J.B., Rathod, P.P., Khatri, B.C., 2016. Investigations on palm oil based biodielectric fluid for sustainable electric discharge machining. In: International Conference on Advances in Materials and Manufacturing (ICAMM-2016).

Valaki, J.B., Rathod, P.P., Sidpara, A.M., 2019. Sustainability issues in electric discharge machining. In: Innovations in Manufacturing for Sustainability. Springer, Cham, pp. 53–75.

Valaskova, K., Throne, O., Kral, P., Michalkova, L., 2020. Deep learning-enabled smart process planning in cyber-physical system-based manufacturing. J. Self Govern. Manag. Econ. 8, 121. https://doi.org/10.22381/JSME8120205.

Wu, K.L., Yan, B.H., Huang, F.Y., Chen, S.C., 2005. Improvement of surface finish on SKD steel using electro-discharge machining with aluminum and surfactant added dielectric. Int. J. Mach. Tool Manufact. 45, 1195–1201. https://doi.org/10.1016/j.ijmachtools.2004.12.005.

Yang, Y., Asiri, A.M., Tang, Z., et al., 2013. Graphene based materials for biomedical applications. Mater. Today 16, 365–373. https://doi.org/10.1016/j.mattod.2013.09.004.